

UNIVERSITÉ DU QUÉBEC EN ABITIBI-TÉMISCAMINGUE

ANALYSE DES CARACTÉRISTIQUES DU CANAL MIMO DANS MINE
SOUTERRAINE

MÉMOIRE

PRÉSENTÉ

COMME EXIGENCE PARTIELLE

DE LA MAÎTRISE EN TÉLÉCOMMUNICAIONS

PAR

ALI NEHME

DÉCEMBRE 2019



BIBLIOTHÈQUE

Cégep de l'Abitibi-Témiscamingue
Université du Québec en Abitibi-Témiscamingue

Mise en garde

La bibliothèque du Cégep de l'Abitibi-Témiscamingue et de l'Université du Québec en Abitibi-Témiscamingue a obtenu l'autorisation de l'auteur de ce document afin de diffuser, dans un but non lucratif, une copie de son œuvre dans Depositum, site d'archives numériques, gratuit et accessible à tous.

L'auteur conserve néanmoins ses droits de propriété intellectuelle, dont son droit d'auteur, sur cette œuvre. Il est donc interdit de reproduire ou de publier en totalité ou en partie ce document sans l'autorisation de l'auteur.

Warning

The library of the Cégep de l'Abitibi-Témiscamingue and the Université du Québec en Abitibi-Témiscamingue obtained the permission of the author to use a copy of this document for non-profit purposes in order to put it in the open archives Depositum, which is free and accessible to all.

The author retains ownership of the copyright on this document. Neither the whole document, nor substantial extracts from it, may be printed or otherwise reproduced without the author's permission.

Acknowledgment

I would like to express my sincere appreciations and gratitude to my directors Prof. Nahi Kandil and Prof. Nadir Hakem. I had the honor to work with them, our fruitful discussions have yielded successful ideas, they are well-known in both experimental and theoretical research. Their valuable knowledge, experience, comments, and suggestions have improved different aspects of my Master thesis. Throughout my M.S, they have been a great role model for conducting research, writing skills, and technical presentations. Many thanks to them.

TABLE OF CONTENTS

Acknowledgment	II
TABLE OF CONTENTS.....	III
LIST OF FIGURES	VII
List OF ABBREVAITATIONS.....	IX
ABSTRACT.....	XI
CHAPTER I.....	1
INTRODUCTION	1
1.1 Motivation.....	1
1.2 Research Problematic.....	2
1.3 Previous Efforts to Design Antenna Configuration in Tunnel Environments	2
1.4 Proposed Solutions.....	4
1.5 Research Objectives and Hypothesis	5
1.6 Contribution and Publication	5
1.7 Structure of the Thesis.....	6
1.8 Adopted Methodology.....	7
CHAPTER II.....	9
OVERVIEW OF MIMO AND DIVERSITY TECHNIQUES	9
2.1 Introduction.....	9
2.2 Principle Characterization of MIMO Based Systems	9
2.2.1 Causes of Fading.....	11
2.2.2 Additive White Gaussian Noise (AWGN):	12
2.2.3 Singular value decomposition (SVD):.....	13

2.2.4 Water-Filling Method:	13
2.2.5 Channel State Information (CSI):	14
2.2.6 Ergodic Capacity	15
2.2.7 Angular Spread and Coherence Distance:	15
2.3 MIMO Categories:	17
2.3.1 Spatial diversity	17
2.3.2 Closed-loop spatial multiplexing	23
2.4 Transmitting Beamforming Analysis	24
CHAPTER III	26
MODAL ANALYSIS OF ELECTROMAGNETIC WAVE PROPAGATION IN UNDERGROUND MINES	26
3.1 Introduction	26
3.2 Related Works of Channel Modeling in Waveguides	27
3.2.1 The Waveguide Model:	28
3.2.2 Geometrical Optical Model (Ray Tracing):	29
3.2.3 Hybrid Model:	30
3.3 Modal Analysis of Lossy Waveguide Environments	31
3.3.1 Multi-Mode Propagation in Lossy Waveguides	31
3.3.2 Theoretical approach for determining the number of modes	33
CHAPTER IV	36
PERFORMANCE ANALYSIS OF SUITABLE MIMO DOWNLINK SYSTEMS IN UNDERGROUND MINE	36
4.1 Introduction	36
4.2 MIMO Antenna Alignment	37

4.3 System Model:.....	38
4.4 Theoretical Results:.....	39
4.4.1 Diversity Techniques Results Discussion:	39
4.4.2 MIMO Antenna Alignments Results Discussion:	43
4.5 Conclusion.....	46
CHAPTER V	47
ANALYSIS OF MIMO CHANNEL CHARACTERISTICS IN LOSSY WAVEGUIDES	47
5.1 Introduction.....	47
5.2 Theoretical Approach.....	47
5.2.1 MIMO Capacity.....	47
5.2.2 Performance Reduction Factors in Tunnels.....	48
5.2.3 Degenerated Channels	50
5.3 System Model and Theoretical Validation.....	52
5.3.1 Effects of Changing Dimensions of the Tunnel Results:.....	52
5.3.2 Effects of Increasing Antennas on Capacity and Power Results:.....	54
5.4 Estimating the Number of Modes in Underground Mine Tunnel:	57
5.4.1 Simulation Setup:	57
5.4.2 Straight Tunnel	58
5.4.3 H-bend Tunnel	58
5.5 Results Discussion:	59
5.6 Conclusion:.....	60
CHAPTER VI	61
CONCLUSION.....	61

6.1 Contributions	61
6.2 Future work	62
APPENDIX A.....	63
NARROW BAND ASSUMPTION IN WIRELESS CHANNEL MODELING	63
REFERNECES	64

LIST OF FIGURES

FIG. 1.1 <i>UCA AND ULA MIMO ANTENNA CONFIGURATIONS</i>	4
FIG. 1.2 PROCESS FOLLOWED TO OBTAIN THE ESTIMATED FORMULA.	8
FIG. 2.1 A $N_{T_x} \times N_{R_x}$ MIMO CHANNEL, HIGHLIGHTING HOW TRANSMITTED SIGNAL....	10
FIG. 2.2 A MULTIPATH PROPAGATION ENVIROMENT REPRESENTING REFLECTION.....	11
FIG. 2.3 POWER AZIMUTH PROFILES COMPARISON BETWEEN CHANNEL	16
FIG. 2.4 SCHEME REPRESENTING THE THREE PRECODING'S MRC,SC,EGC.....	23
FIG. 3.1 DIFFERENT HYBRID MODE SHAPES	29
FIG. 3.2 RECTANGULAR WAVEGUIDE.....	35
FIG. 4.1 CANMET SCHEME AND CANMET MINE IMAGE	39
FIG. 4.2 CAPACITY FOR DIFFERENT MIMO SCHEMES VS DISTANCE.....	41
FIG. 4.3 CAPACITY FRO DIFFERET MIMO SCHEMES IN CDF FOR 900 MHZ.	41
FIG. 4.4 CAPACITY FOR DIFFERENT MIMO SCHEMES IN CDF FOR 2.4 AND 5.8 GHZ	41
FIG. 4.5 SINR VS DITANCE BETWEEN DIFFERET MIMO SYSTEMS FOR 900 MHZ.....	42
FIG. 4.6 POWER VS DISTANCE BETWEEN DIFFERENT MIMO SYSTEMS FOR 900 MHZ.....	42
FIG. 4.7 POWER VS DISTANCE BETWEEN DIFFERETN MIMO SYSTEMS FOR 2.4 GHZ	43
FIG. 4.8 POWER VS DISTANCE PLOT IN THE NLOS PART FOR 900 MHZ	44
FIG. 4.9 POWER VS DISTANCE PLOT IN THE NLOS PART FOR 2.4 GHZ AND 5.8 GHZ.....	45

FIG. 4.10 CAPACITY OF DIFFERENT MIMO ANTENNA ALIGNMENTS FOR THE 900 MHz	45
FIG. 4.11 CAPACITY OF DIFFERENT MIMO ANTENNA ALIGNMENTS FOR 2.4GHz.....	46
FIG. 5.1 ANGULAR SPREAD VS DISTANCE IN CANMET.....	49
FIG. 5.2 CANMET SCHEMATIC.....	52
FIG. 5.3 MEAN NUMBER OF MODES IN CANMET FOR CASE I AND CASE II.....	53
FIG. 5.4 MEAN NUMBER OF MODES IN CANMET FOR CASE I AND CASE II (2.4 GHz) ...	53
FIG. 5.5 MEAN NUMBER OF MODES IN CANMET FOR CASE I AND CASE II (5.8 GHz)....	54
FIG. 5.6 POWER VS DISTANCE BETWEEN DIFFERENT MIMO SYSTEMS (900 MHz).....	55
FIG. 5.7 POWER VS DISTANCE BETWEEN DIFFERENT MIMO SYSTEMS (5.8 GHz).....	56
FIG. 5.8 CDF OF DIFFERENT MIMO SYSTEMS FOR 2.4 GHz.....	56
FIG. 5.9 CDF OF DIFFERENT MIMO SYSTEMS FOR 5.8 GHz.....	57
FIG. 5.10 CURVED TUNNEL SCHEME	59
FIG. 5.11 ESTIMATED VS EXACT NUMBER OF MODES AT A MINE WITH 3 METERS.....	60

List OF ABBREVAITATIONS

AGWN	Additive-Gaussian-White-Noise
AS	Angular Spread
BER	Bit Error Rate
BS	Base Station
CDF	Cumulative Density Function
CSI	Channel State Information
dB	Decibels
EGC	Equal Gain Combining
EM	Electromagnetic
GO	Geometrical Optical Model
GPU	Graphics Processing Unit
LOS	Line of Sight
LTE	Long Term Evolution
MIMO	Multiple Input Multiple Output
MPE	Multi Path Environment
MRC	Maximum Ratio Combining
MRT	Maximum Ratio Transmission
NLOS	Non line of Sight
PDP	Power Delay Profile
SC	Selection Combining
SINR	Signal-to-Interference-plus-Noise Ratio
SISO	Single Input Single Output
SNR	Signal to Noise Ratio
SNR	Signal-to-Noise Ratio
SVD	Singular Value Decomposition
TE	Transverse Electric
TEM	Transverse Electro Magnetic

TM	Transverse Magnetic
TTA	Through the Air
TTE	Through the Earth
TTW	Through the Wire
UCA	Uniform Circular Antenna
UHF	Ultra High Frequency
ULA	Uniform Linear Antenna
VLF	Very Low Frequency
ZF	Zero-Forcing

ABSTRACT

Short-range wireless communications technology has been embraced by the underground mining community in the last few years as a critical part of their method for enhancing the security and productiveness of their operations. In this work, we will demonstrate how the deployment of modern wireless communication systems, primarily based on MIMO antenna array technology will be affected in unique environments like underground gold mines. This work first explores the relation between the number of modes in a lossy waveguide environment and a Multiple-Input Multiple-Output antenna array size. Besides, knowing that beamforming for Massive MIMO is not suitable for deployment in underground mines. We demonstrated that applying beamforming in waveguide-like structures can enhance the performance and that by choosing the appropriate precoding techniques at the transmitter and receiver. Then, in order to achieve more reliability to the MIMO channel, a theoretical study obtained in mine comparing the capacity and power for different antenna configurations. Finally, we estimated the number of propagating modes in a rectangular cross-sectional mine environment and express it as a closed-form function of excitation frequency and waveguide cross-sectional dimensions and length. The presented formulas can be used to estimate the number of modes in the given shape quickly. By applying those previous methods before deploying the wireless communication system in mine, engineers can save time and cost. Besides, they can achieve the highest capacity within the implemented environment by building a wireless channel which is suitable for their desired frequency band.

Keywords: MIMO; estimation; ray tracing; underground mine tunnel.

RÉSUMÉ

La technologie de communication sans fil à courte portée a été adoptée par la communauté minière souterraine au cours des dernières années comme un élément essentiel de sa méthode visant à améliorer la sécurité et la productivité de ses activités. Dans le présent travail, nous démontrerons comment le déploiement de systèmes de communication sans fil modernes, principalement basés sur la technologie de réseau d'antennes MIMO, sera affecté dans des environnements uniques comme les mines d'or souterraines. Ce travail explore d'abord la relation entre le nombre de modes dans un environnement de guide d'ondes déficitaire et la taille d'un réseau d'antennes à débit multiple à entrées multiples. En outre, sachant que la formation de faisceaux pour massive MIMO n'est pas approprié pour le déploiement dans les mines souterraines. Nous avons démontré que l'application de la formation de faisceaux dans des structures semblables à des guides d'ondes peut améliorer les performances et qu'en choisissant les techniques de précodage appropriées à l'émetteur et au récepteur. Ensuite, pour un canal MIMO dans un environnement minier, un résultat théorique obtenu pour différentes configurations d'antennes. Enfin, nous avons estimé le nombre de modes de propagation dans un environnement rectangulaire de la mine transversale et l'exprimons comme une fonction de forme fermée de fréquence d'excitation et de dimensions et de longueur transversales du guide d'ondes. Les formules présentées peuvent être utilisées pour estimer rapidement le nombre de modes dans la forme donnée. En appliquant ces méthodes antérieures avant de déployer le système de communication sans fil dans le mien, les ingénieurs peuvent économiser du temps et des coûts. En outre, ils peuvent atteindre la capacité la plus élevée dans l'environnement mis en œuvre en créant un canal sans fil adapté à la bande de fréquence souhaitée

Mots-clés : MIMO; estimation ;ray tracing; tunnel de mine souterrain.

CHAPTER I

INTRODUCTION

1.1 Motivation

The Mining industry in Canada contributed 57.6 \$ billion to Canada's Gross domestic product (GDP) in 2016 with more than 3700 companies working in this field, employing more than 403,000 workers across the country [1]. These mineral resources are considered as the main blocks in our daily life, where copper and aluminum needed to carry electricity to our homes, and gold which exists in each mobile phone or computer to the lead, zinc, nickel, cadmium, or lithium which are used in batteries. Indeed, following the underground recent mining accidents, the development of a reliable communication system in underground mine has become a paramount need to ensure the safety of miners by providing communication between workers and by providing tracking to accelerate the production by maintaining an excellent safety level. Recently, multiple input multiple output (MIMO) had been embraced by the underground mining community, which has received unprecedented attention due to its reliability and capacity compared to single antenna transmission. However, MIMO can be more complicated compared to single input single output (SISO) antenna system, especially in waveguide like environments where the electromagnetic waves propagation is very complicated. Accordingly, the deployment of the MIMO system can be more productive by studying the relation between MIMO antennas and lossy waveguide environments.

1.2 Research Problematic

First systems established in mines was the digital through the earth (TTE) communication system that was developed by Los Alamos National Laboratory , this system uses very low frequency (VLF) transmission which can penetrate through rocks and huge materials, this communication method was terminated in 1940 with the occurrence of the through the wire technology (TTW), the reason is that this method uses bulky equipment's and lack of speed in data rate. In the late of 1950's, TTW was introduced in mines in order to increase the data rate based on VHF-FM systems. Upon this medium's leaky feeder is considered the suitable solution compared to other cables because it considered as radiating cable the specification that other medium misses. Legacy communication systems such as leaky feeders still exist in underground mines, the deployment of such systems can be costly and they don't have the adequate data rate for modern communication requirements in such environments [2,3]. The modern era of underground mine communication systems began with the through the air technology (TTA) and that because of the need of high data rate communication systems. Indeed, MIMO didn't perform as it supposed to be in free space and that's because EM spread in confined tunnels differs from free space and indoor conditions, where the propagation can be similar to the propagation in waveguide structures. However, the high dependency of such MIMO-based systems on the surrounding physical environment necessitates the characterization of the propagation channel before deployment, else we can't leverage from the MIMO reliability in the confined environments.

1.3 Previous Efforts to Design Antenna Configuration in Tunnel Environments

Before analyzing the MIMO channel in our designated environment, first, we shall examine what the previous studies have yielded concerning different antenna properties in a similar environment such as metro tunnels. Here, the main antenna properties that are taken into account in system designs and deployments for indoor areas are discussed.

Which in terms will introduce the flexibility in the practical design of the wireless communication systems. In this section, we will shed light on radiation pattern, polarization, array configuration, and spacing between the MIMO array elements. For radiation pattern, previous studies focused on coverage and interference; for example, using directive antennas can increase the coverage and reduce the interference. However, the disadvantage is that the performance of the directional antenna is highly dependent on the antenna orientation whereas optimum orientation itself is dependent on the layout of the environment and propagation scenario [4,5]. The performance of omnidirectional disc and directional patch antennas can perform better in an indoor environment, in a study done in [6], omnidirectional antennas gave less mutual inductance compared to directive antennas in a metro tunnel. Hence, we can interpret that beamforming can't perform well in a confined environment. Unlike conventional indoor environments where different antenna polarizations behave equally, outdoor environments such as city urban, they behave differently, and the main reason is due to the ground effect. However, in hallways environments, horizontally polarized waves attenuate more quickly than vertically polarized waves, but they both attenuate at about the same rate in the indoor environment. The main reason behind this effect is due to the Brewster angle phenomena which happen in the interaction of horizontally polarized waves with dielectric sidewalls. The effect of antenna polarization has been studied for SISO and MIMO systems in tunnels too. The main result of the studies for SISO is that in empty tunnels with a horizontal aspect ratio (i.e., width is larger than height), attenuation of the horizontal polarization is lower in any environment. However, this case is true for MIMO systems deployed in underground mines and for an NLOS case. For the LOS case, it's been observed that vertically polarized show lower attenuation, and thus are more desirable for a tunnel without curvatures. In spite of the dissimilarities between underground mines and tunnels, some of our results confirm and support results obtained in subway tunnels. Nevertheless, because underground mines are geometrically diverse, more measurement campaigns in various mines are required to reconfirm previous findings and reveal new physical trends or principles. All the

previous points we discussed can determine the correlation between antenna elements. In addition, two essential factors that can change the correlation level is the antenna spacing and alignment, according to a previous study done by the University of Lille in France in a metro tunnel for a GSM frequency showed that the best antenna alignment can be orthogonal to the tunnel axis with a spacing distance between antennas varying from 2λ to 3λ to ensure decorrelation between the antennas, knowing that in indoor or free space environment the optimal antenna spacing is generally $\frac{\lambda}{2}$. However, considering the differences between metro tunnel and underground mine, in this paper we tested the circular alignment with a smaller separation distance, and that because a 3λ spacing distance in a narrow tunnel can't be sufficiently effective especially when we have UCA [6].

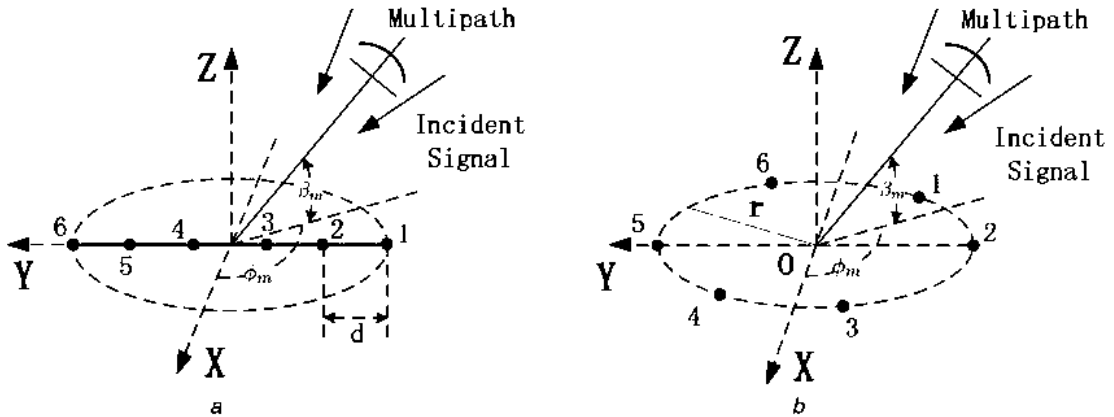


Fig. 1.1: UCA and ULA MIMO antenna configurations.

1.4 Proposed Solutions

In our study, in order to enhance the performance of MIMO in confined environments. We need to determine the optimal precoding method that can work in a low AS environment. Secondly, we need to study the relation between MIMO antennas and

lossy overmoded waveguides like underground mines. Besides, we propose to change the antenna characteristics like spacing, alignment, number of antennas, and polarization of the MIMO antennas in order to limit the correlation between the transmitted signals. In addition, limiting the number of the MIMO array can save complexity and give optimal performance.

1.5 Research Objectives and Hypothesis

We aim to design a MIMO system that can achieve the highest capacity within the implemented environment. In addition, we seek to determine the adequate antenna array size that suits the tunnel cross-sectional area and that by determining an estimate equation that is based on frequency and tunnel dimensions. In our study, we consider that mines can act as tunnels in case of comparing them to over-sized dielectric waveguide where many modes can propagate [7], and this if we consider embracing the waveguide model, but the problem with the latter that it's not efficient in the near field region, where the geometrical optical model (GO) can numerically solve the problem of the near field region by predicting the paths [8]. Correspondingly, we can use GO model which is more precise in undefined shapes like underground mines. In this manner, we can use the right channel modeling which facilitates the design of such systems to answer questions such as “what is the suitable antenna alignment, frequency do we need?” or “What channel impairments do we need to mitigate?”

1.6 Contribution and Publication

1- Nehme, A. Kandil, N et Hakem, N., "Estimating the number of modes in underground mine tunnel", 2019 IEEE International Symposium on Antennas and Propagation (APSURSI).

In this article we explore the relation between number of modes in a lossy waveguide environment and MIMO antenna array size, the aim is to make an estimation of the number of modes in underground mine tunnel. The estimating formulas can be used to determine the number of modes which can propagate in straight mine tunnels.

2- Nehme, N. Hakem, N et N, kandil., "The Effects of Increasing Antenna Arrays for MIMO in Mine Tunnels", 2019 9th International Conference on Digital Information and Communication Technology and its Application (DICTAP2019).

The aim of this paper is to prove theoretically by using waveguide and geometrical optical models that increasing MIMO array elements at the transmitter and receiver will have a limit on capacity where the equivalent spatial subchannels can be limited by the number of allowable modes.

3- Nehme, A. Kandil, N et Hakem, N., "Analysis of MIMO Antenna Characteristics in Underground Mine ", 2019 International Conference on Advance of Computational tools for Engineering Applications (ACTEA2019).

"Analysis of MIMO Antenna Characteristics in Underground Mine " summarizes the previous two works, besides it helps answering question such as “what is the suitable antenna alignment and the suitable frequency” for different mine cross-sections.

1.7 Structure of the Thesis

The rest of the thesis is structured as follows:

Chapter II provides some background material about MIMO and introduces important concepts such as the diversity schemes that will be used in chapter IV.

Chapter III, sheds the light on understanding wireless propagation in the mine tunnel. In addition, it presents some mathematical derivations to explain the relation between MIMO channel and lossy overmoded waveguides and it explains the differences between different channel modelling.

In Chapter IV we will use different beamforming techniques such as MRT and ZF to compare their performance in the underground mine. In addition, a comparison between antenna alignments will be studied for several frequencies.

In Chapter V, we will prove mathematically and theoretically that limiting the number of MIMO antennas in narrow mines can achieve the same performance as higher antenna MIMO arrays. In addition, we will estimate the number of modes in several tunnel shapes.

Finally, Chapter VI concludes the thesis by reaffirming our contributions and further studies.

1.8 Adopted Methodology

For the first step, in order to characterize the MIMO channel in a specific environment, we need to study the MIMO systems which in terms require the propagation channel to be correctly characterized or modelled. This characterization is important as it provides a better understanding of propagation phenomena, such as reflection, diffusion and refraction, in any given environment. It's known that for our designated environment that it acts as waveguide when dealing with VHF. Hence determining the number of propagating channels can help in building our estimating formulas and that by conducting massive simulations for various mine environments and different channel

parameters. The chart below shows the approach followed to achieve our proposed solutions.

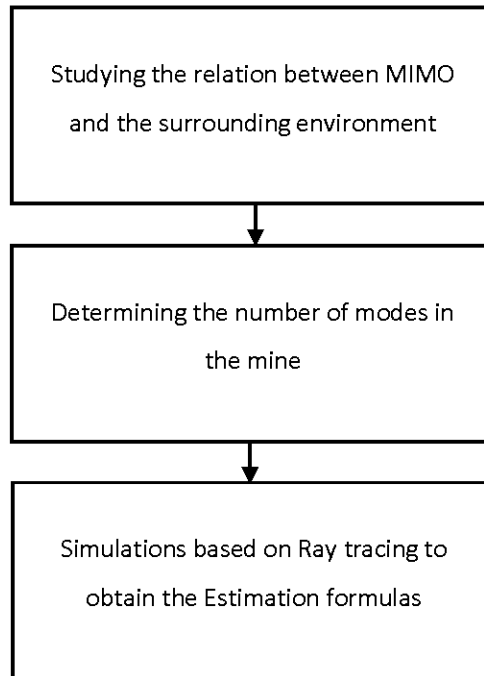


Fig. 1.2: Process followed to obtain the estimating formulas.

CHAPTER II

OVERVIEW OF MIMO AND DIVERSITY TECHNIQUES

2.1 Introduction

Some challenges in wireless propagation are the fading of the signal due to many physical behaviors of waves. As a result, we have multiple single components at the receiver, this multipath propagation environment (MPE) leads to a superposition of multiple signals, which leads to interference that can be destructive or constructive. The challenge faced by future wireless communication systems is to achieve high data rate combined with high-quality service. Knowing that spectrum is a scarce resource, and due to MPE, this requirement calls for means to radically increase spectral efficiency. Indeed, MIMO can overcome these problems without sacrificing additional bandwidth or power. In this chapter, we will briefly shed light on MIMO systems in order to facilitate the idea for the next chapters. Also, we will introduce some MIMO techniques that permit a device that uses a couple of antennas at the transmitter or receiver to take advantage of spatial diversity in order to enlarge the reliability and the throughput of a channel.

2.2 Principle Characterization of MIMO Based Systems

In order to characterize MIMO systems, we must recall two key parameters represented by the angular spread and capacity. Multiple transmission paths in any environment could increase the capacity if we considered treating each path as an independent channel. In tunnels, which is familiarized by its small angular spread, the using of beamforming can be quite different, and that is due to the inability of the receiver to

distinguish between those paths. A solution can be proposed by using diversity techniques which will be discussed in the next subsection. The capacity of a MIMO system can be predicted by considering N_{Tx} transmitting antennas and N_{Rx} receiving antennas, and derived by Shannon's law the formula is given by:

$$C = \log_2 \left[\det \left(I_{N_{Rx}} + \frac{SNR}{N_{Tx}} H_{nor} H_{nor}^* \right) \right] \text{ bits/sec/Hz} \quad (1)$$

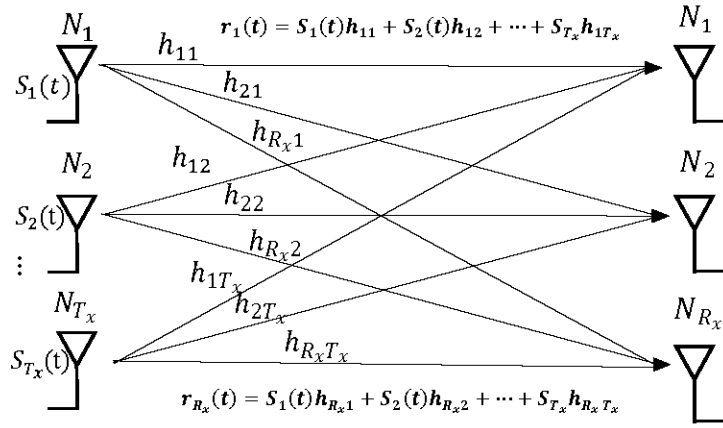


Fig. 2.1: A $N_{Tx} \times N_{Rx}$ MIMO channel, highlighting how transmitted signals are affected in the channel.

where $*$ denotes the transpose-conjugate or the Hermitian, H is the $N_{Rx} \times N_{Tx}$ channel matrix [9]. In order to increase the capacity with respect to the minimum number of transmitting and receiving antennas, the signal fading of the rich multipath environment must be observed individually at the receiving antennas, and we consider this case as a full rank channel matrix. Contrarily, if there is a correlation between paths or if the multiple transmission paths fade dependently, in such case a rank deficient will occur, and the capacity gain will be limited. Before diving into diversity techniques, we must recall some mathematical and physical aspects that will be discussed in the next chapters.

2.2.1 Causes of Fading

In any terrestrial wireless communications system, the signal will reach the receiver not only via the direct path, but also as a result of reflections from objects such as mountains, buildings, ground, water, etc. that are adjacent to the main path. Reflection occurs when waves impinge upon an obstruction that is much larger in size compared to the wavelength λ of the signal. The multipath effect is the main cause of fading which arises from the scattering action of the scatters. Scattering occurs when the radio channel contains objects whose sizes are on the order of the wavelength or less of the propagating wave and also when the numbers of obstacles are quite large. They are produced even by small objects, surface roughness and other irregularities on the channel. It follows same principles of diffraction. Diffraction is a proportional scenario in which an object whose dimension is larger than the signal wavelength and which has sharp edges obstructs a path between transmitter and receiver and cause new secondary waves to be generated (Fig. 2.2).

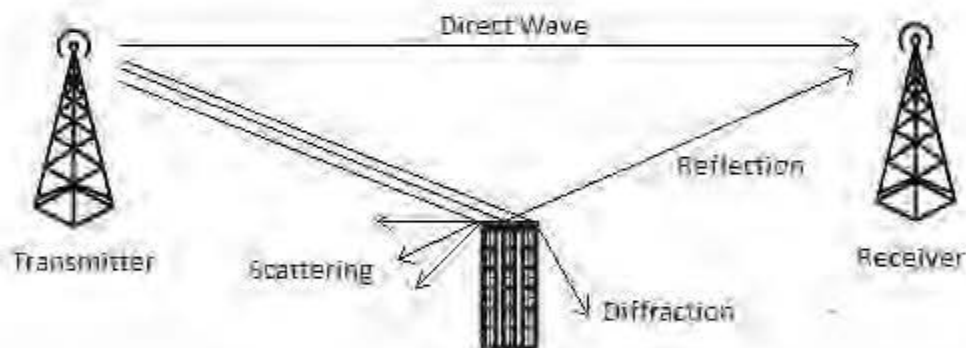


Fig. 2.2. A multipath propagation environment representing reflection, scattering and diffraction of the transmitted signal.

The overall signal at the receiver is a summation of the LOS and NLOS components which lead to superposition of multiple signals which will be either constructive or destructive. Fig.2.2 depicts the multipath echo formation from an actual target. The

wireless channel can be represented mathematically as the summation of multiple signals each has different delay and attenuation as follows:

$$h(t) = \sum_{i=0}^{L-1} a_i \delta(t - \tau_i) \quad (2)$$

where a_i represents the attenuation of each path and τ is the delay that differs according to each signal path.

2.2.2 Additive White Gaussian Noise (AWGN):

Additive white Gaussian noise (AWGN) is basic and generally accepted model for thermal noise in communication channels, it's a model used in Information theory to mimic the effect of many random processes that occur in nature. The modifiers have a set of assumptions that:

- Additive: The noise is additive, i.e., the received signal equals the transmit signal plus some noise, where the noise is statistically independent of the signal.
- White: Refers to the idea that it has uniform power across the frequency band for the information system.
- Gaussian: The noise samples have a Gaussian distribution in the time domain with an average time domain value of zero.

The AWGN channel is an important model for many satellite and deep space communication links. However, for terrestrial path modeling, AWGN is commonly used to simulate background noise of the channel under study, in addition to multipath, terrain blocking, interference, ground clutter and self-interference that modern radio systems encounter in terrestrial operation [10].

2.2.3 Singular value decomposition (SVD):

One of the most useful methods from linear algebra is the matrix decomposition known as the singular value decomposition. It's an important tool for analyzing MIMO systems. The method is to decompose the basic matrix into three matrices. Accordingly, every matrix H can be decomposed accordingly to singular values as follows:

$$H = UDV^H \quad (3)$$

Where the matrices U, V are unitaries of dimensions $n_r \times n_r$ and $n_t \times n_t$, while D is a non-negative diagonal matrix of dimensions $n_r \times n_t$. The diagonal elements of matrix D are the singular values of the channel matrix H . The algorithm of singular value decomposition that provides the above transformation can be found in [11].

2.2.4 Water-Filling Method:

Water-Filling algorithm is a technique used in digital communications systems for efficiently allocates different levels of power to various transmitting antennas or among different channels in multicarrier schemes. This technique proves its optimality for channels having AWGN and Inter Symbol Interference. The algorithm allocates more power to the antennas that experience channels that are in better conditions, and less or none at all, to the antennas whose channels are in bad conditions [12]. If the channel is completely known. Hence, assigning power can be more efficient and in according with the channel conditions the capacity can be improved. Water-Filling method has to satisfy the optimal power allocation policy, since this algorithm only concentrates on good-quality channels and discards the bad ones during each channel realization, it is to be expected that this method yields a capacity that is equal or better than the capacity when the channel is unknown to the transmitter [13].

2.2.5 Channel State Information (CSI):

Channel state information refers to known channel properties of a communication link. For MIMO systems. The transmitter or receiver must have accessibility to instantaneous CSI. This information describes how a signal propagates from the transmitter to the receiver and represents the power decay and the physical aspects that are discussed in the previous section. CSI aims to make a channel estimation, this estimation of the channel allows adapting transmissions to current channel conditions, which is crucial for achieving reliable communication with high data rates in multiantenna systems. The knowledge of accurate and timely CSI at the transmitter is becoming increasingly important in wireless communication systems [14]. While it is often assumed that the receiver needs to know the channel for accurate power control, scheduling, and data demodulation. According to SVD in the previous section, we can express the total capacity of n SISO subchannels as in equation (4):

$$c = \sum_{k=1}^n \log_2(1 + p_k \epsilon_k^2) \quad (4)$$

Where p_k is the power allocated to the k th subchannel and ϵ_k^2 is the eigenvalues of the HH^H matrix. From this perspective, the transmitter might have a knowledge of the CSI or might not. If the transmitter doesn't have knowledge of the CSI, in this case, the transmitting signal s is chosen to be statistically non-preferential, which implies that the n_t components of the transmitted signal are independent and equi-powered at the transmit antennas [15]. Hence, the power allocated to each of the n_t subchannels is $p_k = \frac{p}{n_t}$. Applying the last expression to Equation 1 gives:

$$c = \log_2[\det(I + \frac{p}{n_t} HH^H)] \quad (5)$$

In the case of a known CSI at the transmitter, now waterfilling method can be applied at the transmitter. In this way, the SISO subchannel that contributed to the highest data rate is supplied with more power.

2.2.6 Ergodic Capacity

The ergodic capacity of a MIMO channel is the aggregate average of the information rate over the distribution of the elements of the channel matrix H , and it is given by:

$$C = E\{I\} \quad (6)$$

When there is no CSI at the transmitter, we can substitute Equation (6) into Equation (1), so the ergodic capacity is given by:

$$c = E\{\log_2(\det(I + \frac{p}{n_t} HH^H))\} \quad (7)$$

Whereas with CSI at the transmitter the ergodic capacity is given by:

$$C = E\{\sum_{k=1}^n \log_2(I + \frac{p}{n_t} \gamma_k \epsilon_k^2)\} \quad (8)$$

Where γ_k corresponds to the amount of power that is assigned to the k th subchannel. The goal with the waterfilling algorithm is to find the optimum γ_k that maximizes the capacity given in (8), where p_k is the power allocated to the k th subchannel and ϵ_k^2 is its power gain, where p is the maximum normalized transmit [16].

2.2.7 Angular Spread and Coherence Distance:

Moving to angular spread, path loss and delay spread are the main channel characterization which SISO systems focuses on. However, its known that spatial

domains become equally important as the temporal domain for MIMO systems. Hence, power azimuth spectrum (PAS) has been defined, which determines the spatial distribution of the received power over the degrees of freedom in the horizontal domain (azimuth domain) [17]. In the 2D structured antenna array, one can control the radiation beam pattern to provide more degrees of freedom in supporting users on both vertical which represents the elevation angle and horizontal which represents the azimuth angle direction so that the control of the transmit beam is in 3D. In our study, we considered only the azimuth angle since our environment is designated to have a limited height across its cross-sectional dimensions. Fig. 2.3 supports this approach, in this experiment that's done by Yin and Zheng in Nantong tunnel, China [18]. We can interpret that the angular spread in the smaller distance separation between the T_x and R_x is wider comparing to a larger distance. This phenomenon leads us to two crucial points in our study. First, propagation in like these environments can be separated into two regions, the near-field and the far-field region, which the free space propagation principals can be applied in the near-field region. The other point is that as the R_x is located farther from the T_x point, the angular spread will drop eventually which will lead the propagation to act similarly as a waveguide.

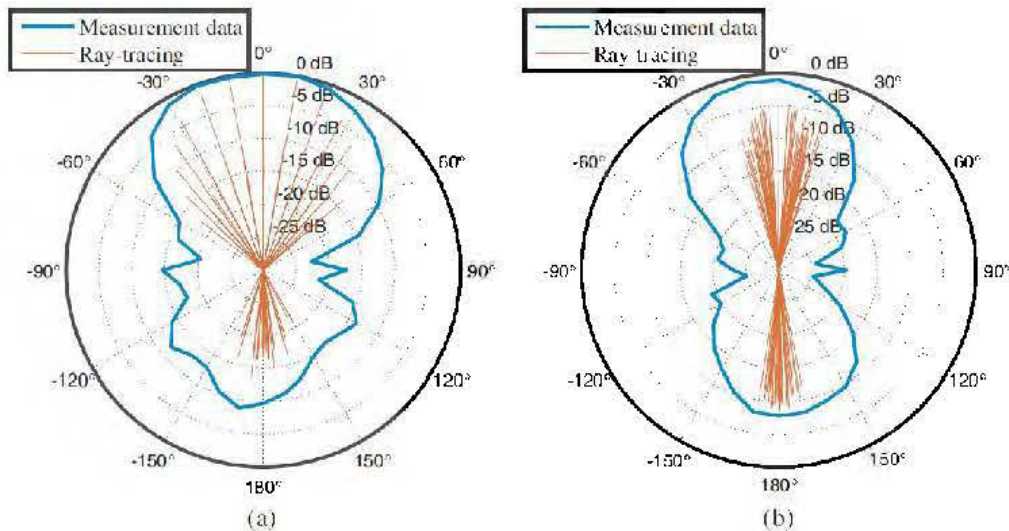


Fig. 2.3: Power Azimuth Profiles comparison between channel measurement and ray-tracing simulation in Nantong tunnel. (a) Co-polarized and Tx-Rx distance 25m. (b) Co-polarized and Tx-Rx distance 75 m [18].

Indeed, a parameter that characterizes selective space fading's is the coherence distance, the coherence distance D_c is the spatial distance over which the channel does not change appreciably. It is a common and important wireless communication channel parameter, D_c that is inversely proportional to the angular spread. The D_c is the spatial separation for which the autocorrelation coefficient of the spatial multiplexing drops to

0.7. In conventional indoor and microcell environments, the PAS at the mobile unit tends to be broad so fading on adjacent antenna elements tends to be more uncorrelated for relatively small element separations. Linear confined spaces such as tunnels and drift in underground mines tend to function as overmoded waveguides at radio frequencies. As a result, the PAS in such environments are expected to be considerably narrower than in conventional environments and the performance of MIMO wireless systems, is likely to be reduced [15].

2.3 MIMO Categories:

In principle, MIMO offers three different benefits, namely spatial diversity, spatial multiplexing, and beamforming gain [19]. This chapter describes the difference in performance for each MIMO technique in an underground mine and by obtaining the impact of those techniques on the capacity, power, and SINR at the receiver array. (SINR is a measure of signal, interference and noise quantity in a wireless system. It indicates how much desired signal is stronger compare to Noise and interference).

2.3.1 Spatial diversity

Due to Severe attenuation in a multipath wireless environment, the receiver can't retrieve the transmitted signal unless the latter is provided with some form of diversity. Indeed, by transmitting the data signals over multiple independently fading dimensions

in frequency, time, and space and by performing proper combining at the receiver, in this case, we can achieve diversity gain.

The method is to provide the receiver with less-attenuated replica of the transmitted signal. In some applications, the only practical means of achieving diversity is the deployment of antenna arrays at the transmitter and/or the receiver. However, considering the fact that receivers are typically required to be small, it may not be practical to deploy multiple receive antennas at the remote station [18]. This motivates us considering transmit diversity. So, Applying received spatial needs a signal processing at the receivers, and for small devices, it will be not desirable, instead of transmitted spatial is more preferable.

Diversity is introduced in its different forms to enhance the performance of the system. Time diversity where the same message is being transmitted at different time slots, frequency diversity the same message is being transmitted at different frequencies and space diversity that uses separate antennas located in different positions to take advantage of the different radio path [20]. To demonstrate the benefit of diversity we must know that the received signal can be represented as the sum of the various multipath components as follows:

$$y_p(t) = \sum_{i=0}^{L-1} \text{Re} \{a_i(t) s(t - \tau_i) e^{j2\pi f_c(t - \tau_i)}\} \quad (9)$$

Where a is the attenuation of each path and s is the transmitted signal at certain time t and τ is the delay, and f_c is the carrier frequency. Considering taking the baseband received signal only and applying the narrow band assumption for the transmitted signal, we will have the following equation:

$$y_p(t) = \sum_{i=0}^{L-1} a_i(t) s(t) e^{-j2\pi f_c \tau_i} \quad (10)$$

The detailed deduction of the previous equations is provided in Appendix A. The impulse response of the channel becomes:

$$h(t) = \frac{y(t)}{s(t)} = \sum_{i=0}^{L-1} a e^{-j2\pi F_c \tau_i} \quad (11)$$

Where $h(t)$ follows Rayleigh distribution. Although Rician distribution is more used for LOS situations, but Rayleigh can be more accurate in mines where the signals can rave because of the mine curvatures. Besides, having static simulations with independent channel realizations can neglect the LOS or NLOS consideration. knowing that poor performance in the wireless system can occur if the signal power is less than noise threshold where this situation is assigned to the deep fade of the wireless channel. In addition, BER is proportional to the deep fade where destructive interference occurs. Thus, spatial diversity can solve deep fade situations, now multiple antennas can exist at the receiver and hence decreasing the probability of the deep fade, where the BER can decrease with increasing the spatial elements as follows [21]:

$$BER = \left(\frac{1}{SNR^L} \right) \quad (12)$$

Where L is the number of antennas, indeed, this is not the case for waveguide-like structures, so by increasing the number of elements, we cannot achieve a low BER as we will see in Chapter IV.

2.3.1.1 Receiver Diversity Techniques:

Received diversity techniques are performed at the receiver to strengthen the signal. These techniques can be applied once two or more channels that have uncorrelated fading are transmitted. Thus, by combining those channels into a single amplified signal

without additive noise, the system's reliability can be improved. In this section we will introduce three main received diversity techniques which will be used in Chapter IV.

i. Maximal ratio combining (MRC):

The main aim of this method is to maximize the SNR at the receiver for the multiple received elements and that by combining the received voltages by using a weighting vector which can adjust both the magnitude and the phase, the receiver optimally combines the received voltage from all antenna elements using a weighting vector that adjusts both the phase and the magnitude (Fig.2.4). The general model for MIMO wireless communication is given as [22]:

$$\begin{aligned} y &= Hx + n \\ &= HPs + n \end{aligned} \quad (13)$$

Where $x = Ps$ is the precoded and $r = Wy$ is the filtered output.

In the maximal ratio combining, all received signals are coherently combined at the receiver, e.g.:

$$r = w^H y = w^H h x + w^H N \quad (14)$$

Where the optimal weighting vector w maximizes the moutput SNR for the intended user by Cauchy-Schwartz inequality it is found that SNR is maximized when w is proportional to h as follows:

$$\gamma = \frac{|w^H h|^2}{E|w^H n|^2} = \frac{|w^H h|^2}{\sigma^2 E|w^H W|} \quad (15)$$

$$w = \frac{h}{norm} \quad (16)$$

Where H is a normalization factor that scales the weighting vector such that the sum of the squares of the magnitudes is equal to N_r . This weighting vector is then applied to the h -vector to compute the total received power.

ii. Selection combining (SC):

The basic idea in SC is to choose the branch which have the highest SINR. To calculate this, each receiver antenna should be treated as if it were an individual receiver (Fig. 2.4). From channel gain, the received power for receiver antenna element, k is calculated as follows:

$$p_{r_k} = \frac{P_t}{N_t} |h_k|^2 \text{ mW} \quad (17)$$

Where P_t is the total transmitter power in milliwatts, and N_t is the number of transmitter antennas over which this power has been divided. The same equation can be used to calculate the interference power to this antenna using the corresponding h -vectors from transmitters identified as interferers. SINR is then calculated for each receiving antenna, and the highest is selected. The capacity, throughput, and BER can then be calculated from this SINR value as if this were a SISO antenna [14].

iii. Equal gain combining (EGC):

EGC is considered to be simpler and cheaper for practical implementation than MRC, and that because all summands have the same weighting factor, by applying a weighting vector to align phases before combining the channel gains from each receiver antenna (Fig. 2.4), it will not be required to measure and estimate SNR in all the diversity

branches. But we can expect from this simplicity that MRC can perform better, especially in a rich scattering environment. To calculate the total received power, a weighting vector is calculated that has unity gain and a phase equal to that of the h vector for each element [15,16]:

$$W_k = e^{j\angle h_k} \quad (18)$$

This weighting vector is then applied to the h -vector for the receiver elements to compute the total received power:

$$P_r = \frac{p_t}{N_t} |w^T h|^2 = \frac{P_t}{N_t} \left[\sum_{k=0}^{n_R-1} |h_k| \right]^2 \quad (19)$$

Where the superscript “T” denotes the Hermitian transpose of the weighting vector.

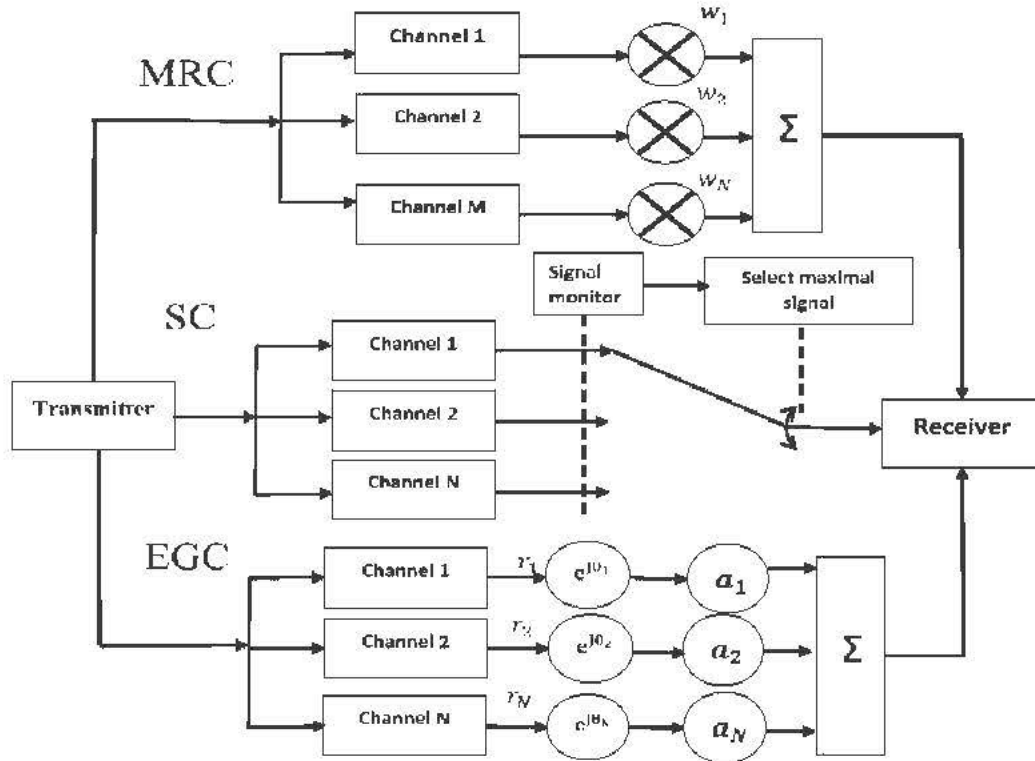


Fig. 2.4: Scheme representing the three precoding's MRC, SC and EGC.

2.3.2 Closed-loop spatial multiplexing

The second MIMO method is Closed-Loop Spatial Multiplexing uses Singular Value Decomposition (SVD) to calculate precoding weights applied at the transmitter and combining weights at the receiver to generate multiple, non-interfering, data streams. For throughput calculations, the total throughput is calculated by summing the individual throughputs of each stream. For other communication system outputs, the best value from all streams is returned. Similarly, for interference and noise analysis, the highest SNR and SINR of all generated data streams is returned. In which the transmitter and receiver coordinate to generate an optimal set of independent data streams. This method uses the SVD technique, for a single user, this provides multiple,

independent streams (diagonals of the Σ matrix) that can each contribute to the total throughput or capacity.

Once the precoding and post-process matrices, U and V , have been applied, the equivalent channel matrix can be described by the singular value matrix Σ instead of H according to the following equation:

$$\Sigma = U^T(U\Sigma V^T)V = U^T H V \quad (20)$$

This matrix has the same dimensions as H , $N_r \times N_t$, but contains values only along the diagonal for a number of singular values equal to the minimum of the two dimensions of the matrix, N_r and N_t .

2.4 Transmitting Beamforming Analysis

Beamforming or spatial filtering is a signal processing technique used in different areas from MIMO, to massive MIMO, to interference mitigation or wireless sensor networks. The aim of beamforming is to use sensor arrays at both the transmitting or receiving ends in order to achieve spatial selectivity and that's by directing the signal. This is achieved by combining elements in an antenna array in such a way that signals at particular angles experience constructive interference while others experience destructive interference. Directing signals may be applied only from one side, for example transmission beamforming concentrates the transmitter to the direction of the mobile receiver, this situation is our concern in this chapter. In this study we will consider two types for transmitting beamforming: the first is an adaptive technique called maximum ratio transmission (MRT) and the second is zero-forcing technique (ZF). Beamforming techniques such as MRT and ZF which is based on knowing the CSI channel cannot be very effective in waveguide like environments, and that is related to the coupling between the channels. However, in mine tunnel which have unperfect

walls the situation can be a quite different. MRT, as the name implies, intends to maximize the SNR. It is the easiest method from a signal processing perspective, as the detection/precoding matrix is only the conjugate transpose or conjugate of the CSI matrix, H . The significant downside of this method is that inter-user interference is disregarded. In brief, this technique uses the channel matrix within the transmitting and receiving antennas to optimize the power at the receiver [21]. The beamforming weighting matrix between a transmitter and a particular receiver antenna element, k , is defined as:

$$w_k = \frac{h_k^t}{|h_k|} \quad (21)$$

Where h_k is the N_t channel vector between the transmitting array and the receiver antenna. The quantity in the denominator is the absolute magnitude of the channel vector, which is the square root of the sum of the square magnitudes of the channel vector. This weighting matrix maximizes the beam to the specific receiver antenna.

In the other side, ZF precoding strives to inscribe the inter-user interference problem by designing the optimization guidelines to reduce it. The detection/precoding matrix is the pseudoinverse of the CSI matrix. Determining the pseudoinverse is more computationally costly than the complex conjugate as in the MR case. Yet, by focusing so keenly on reducing the interference, the received signal at the user suffers from the lack of power.

CHAPTER III

MODAL ANALYSIS OF ELECTROMAGNETIC WAVE PROPAGATION IN UNDERGROUND MINES

3.1 Introduction

While previous studies of MIMO modeling and configuration design in confined spaces have yielded useful insights, they cannot replace studies that is designated for underground mines. Consequently, undergrounds communication engineers have had little to guide them as they seek to design and deploy MIMO based wireless systems. Compared to transportation tunnels (the most similar to the mine tunnels), whereas MIMO is considered to be more complicated compared to SISO especially in underground mine tunnels that have a narrow width which may lead to higher modal cut off frequencies and lower angular spread that will cause a limitation to the MIMO performance. In addition, mine tunnels have branches, considerably rougher walls, and irregular geometry, which cause much more diffuse scatter. Indeed, further study is required in order to assess the relative magnitude of these effects and to determine the MIMO performance that can be achieved [23].

Consequently, as a result, in this chapter, we will discuss wave electromagnetic propagation in these confined environments in order to assess the performance of

MIMO systems. Besides, a modal analysis in mine tunnels is introduced, and we calculated the number of modes which is necessary to know the propagation channels as we will see in Chapter V.

3.2 Related Works of Channel Modeling in Waveguides

Recently, as technology has migrated toward higher frequencies, channel modeling has become more complex. Previously, in many models, they treat underground tunnels as simple tunnels with smooth walls. Taking an example, the single mode waveguide model which has been proposed 50 years ago can model the propagation loss signals in mine today for the UHF band (200-4000 MHz) [24]. Recent channel modeling versions have been enhanced and customized to treat multimode, which can be more accurate in modeling delay spread and propagation loss in the upper UHF band. Previous work on waveguide propagation have been extended by Emslie et al. in [25] for the rectangular cross sections, by considering them as an oversized dielectric waveguide, and they found accurate mode equations which are based on the simple assumption of uniform dielectric constant for the tunnel. In order to provide more accuracy to the model, Mahmoud and Emslie, and wait in [26] considered dielectric constant of the sidewalls was different from the dielectric constant existed in the floor and the ceiling, this case can be better than considering a uniform dielectric constant. In [27], Emslie et al. applied a waveguide model to tunnels with approximately rectangular cross-section, such as coal mines with a considerable degree of roughness, and tunnels with curved walls.

Currently, there are four main channel models exists for tunnels include the waveguide model, the Geometrical optical model (GO model), the full wave model, and the hybrid model.

3.2.1 The Waveguide Model:

Transmission of EM waves in tunnels under some conditions may take the form of waveguide propagation. For the transmission to take this form, the materials bounding the tunnel must have a dielectric constant ranging between 5 to 10, besides for having a frequency which is above 500 MHz. A waveguide is a structure that guides waves, such as electromagnetic waves or sound, with minimal loss of energy by restricting expansion to one dimension or two, those structures functions as “conduits” for carrying electromagnetic waves. They are practical only for signals of extremely high frequency, where the signal wavelength approaches the cross-sectional dimensions of the waveguide. Electromagnetic waveguides are analyzed by solving Maxwell's equations, or their reduced form, the EM wave equation, including the boundary conditions defined by the characteristics of the materials and their interfaces. These equations have multiple solutions, or modes, which are eigenfunctions of the equation system. Each mode is described by a cutoff frequency under this frequency the mode cannot exist in the guide. Waveguide propagation modes depend on the operating wavelength and polarization and the shape and size of the guide. The longitudinal mode of a waveguide is a particular standing wave pattern formed by waves confined in the cavity. Fig.3.1 shows a graphical depiction of the E field variation in a waveguide for the TE_{10} , TE_{20} , and TE_{30} modes. As can be seen, the first index indicates the number of half wave loops across the width of the guide and the second index, the number of loops across the height of the guide which in this case is zero. The transverse modes are classified into different types:

- TE modes (transverse electric) have no electric field in the direction of propagation.
- TM modes (transverse magnetic) have no magnetic field in the direction of propagation.
- TEM modes (transverse electromagnetic) have no electric nor magnetic field in the direction of propagation.

- Hybrid modes have both electric and magnetic field components in the direction of propagation.

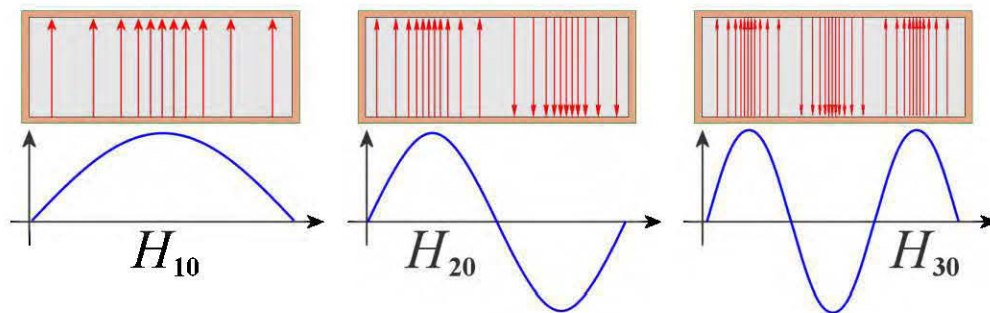


Fig. 3.1: Different Hybrid mode shapes.

3.2.2 Geometrical Optical Model (Ray Tracing):

Unlike modal analysis in the waveguide model, which is restricted to simple geometries, ray-optical methods can be applied to more complex scenarios such as occupied tunnels, tunnels with curvature, the coupling between outside and inside of the tunnel, etc. The name ray tracing is used to describe the process in which the electromagnetic fields are modeled in this method. Applying a high frequency approximation, a transmitting source emits a series of ray tubes in all directions that propagate outwards and represent different points on a wavefront. As the rays travel away from the source, they incur phase change and loss that is associated with an outwardly propagating wave at a given frequency. Interactions with objects are computed based on the Fresnel and diffraction equations that govern geometric optics [28]. There are generally two types of approaches to ray tracing. The first is known as the shooting and bouncing ray (SBR) method which essentially launches a number of

rays in all directions from the source in order to sufficiently illuminate its surroundings [4]. Upon the point of contact with a media boundary, a new set of rays are excited, traveling according to the laws of reflection, refraction, and diffraction. Each ray decays as it propagates and is terminated when its amplitude has dropped below a given threshold. At the receiver point, a reception radius is applied to sum up and average out all the incoming fields that intercept the given area or volume. A very large number of rays is typically required for the fields to converge, and since each ray can branch out exponentially before decaying below the threshold, this method can still be computationally intensive for large environments with many scatterers. However, in some cases, the SBR method is advantageous in the sense that the final result characterizes the entire simulation domain.

For geometrically simpler surroundings, the image theory (IT) method tends to be more efficient as the effects of multiple reflections and refractions are much easier to calculate [4]. Instead of systematically shooting out rays in all directions, the algorithm first calculates, based on the positions of the transmitting and receiving antennas, precisely which rays will propagate to the receiver point. As a result, there is no need for a sampling radius and no time is spent computing ray paths that do not contribute to the field at the receiver because the user chooses which region to illuminate and what areas can be ignored. Its name is taken from the simple example of a transmitter located above a ground plane, in which the resulting reflection is effectively modeled by an image source below the ground generating the reflected fields. In the case of more complicated scenarios there are many more planes and, hence, multiple reflections and many more image source locations to compute, but the concept remains the same.

3.2.3 Hybrid Model:

For arbitrary tunnel shapes, GO and Full wave model can be more accurate in near and far field regions, but this model needs high-performance computers if the tunnel distance is large. For this reason, the hybrid model reveals as a combination of GO model and waveguide model in order to facilitate computer calculations and to solve the near field region precision. The Multimode model was a good innovation in the hybrid model, where the basic idea is to separate the tunnel into two field regions, the far-field region and the near-field region and that is because in a lossy waveguide environment a large number of modes exists near the transmitter where waveguide can't model this case. Thus, the method used is to use the free space model in the near-field and by assigning rays to modes by a matching technique, multimode model is explained in details in [26].

For this work, we adopted the ray-tracing model since our simulations consider taking tunnel with a maximum 200 m length. Indeed, recent graphics cards can bear this simulation with a short time; consequently, we can avoid the complexity of hybrid and full-wave models and with a precise result.

3.3 Modal Analysis of Lossy Waveguide Environments

The aim of this section is to understand how EM wave propagation acts in mine tunnels. In addition, we will demonstrate how to calculate the number of modes in an oversized lossy waveguide.

3.3.1 Multi-Mode Propagation in Lossy Waveguides

In the UHF band, any structure can be modeled as a waveguide if the latter can guide the EM wave through a tunnel shape. Inside the waveguides, EM fields can be resolved into the sum of propagation modes given by resolving Maxwell's equations subject to

the boundary conditions. In the case of dielectric surfaces, propagating waves may be expressed by hybrid modes, with all three cartesian components of the electric and magnetic field present. These modes are lossy modes because any portion of the wave that spread on the guide wall is partially reflected into the surrounding dielectric and partially reflected back into the waveguide, the refracted component propagates away from the waveguide and represents a power loss [29]. By identifying tunnel dimensions and material, Maxwell's equations subject to boundary conditions generated by the interfaces between the interior of the tunnels and the wall materials, determine the propagation constant, cutoff frequency and propagation loss for each mode.

These are important environmental parameters for wireless designs in lossy waveguides such as underground mines. Mine tunnels also may act as a waveguide, resulting in a path loss exponent less than 2. Path loss exponent is a measure that yields to what power of separation the signal power in the profile decays. It can be determined by applying regression analysis. Most of path loss models have one or more several breakpoints which distinguish areas where radio wave experience different path loss exponents. In some environments such as buildings and other indoor environments, the path loss exponent can reach values in the range of 3 to 6. Tunnel path loss model has also breakpoints which separate far-field and near field regions. The breakpoint location in a tunnel depends on the largest cross-sectional dimensions (width or high) of the tunnel relative to the signal wavelength. It should be noted that the far-field and near-field definitions for propagation models in tunnels are not the same as far field and near field of an antenna. Near field region of a straight tunnel is considered the region before the breakpoint wherein the cross-sectional plane where the transmitter is located, the antenna excites multiple modes. Each mode has a different intensity and phase. In this region, the signal fluctuation is significant because of the reflections and multipath components coming from different directions. Indeed, the waveguide suffers a larger loss than far-field propagation [30, 31]. This is because the higher order modes are significant in the near-field and should be included in calculations. After the breakpoint,

higher order modes are greatly attenuated and considered to be evanescent modes at large distances and that because of the high attenuation factor they have, and this attenuation results from impinging the walls within a grazing angle, while the fundamental modes survive and they contribute to the total power at the receiver. The separation breakpoint between these two fields is still hard to be obtained in a direct manner due to the different environment shapes, for UHF band which is considered to be higher than the cut off frequency of the waveguide, the near field is prolonged, or we can say that the breakpoint is extended from the transmitter, so in this case high order modes can't be neglected because they contribute heavily to the receiver power in the near field zone [28,29].

3.3.2 Theoretical approach for determining the number of modes

In order to determine the number of modes in any arbitrary rectangular cross-section waveguide we must consider some parameters such as frequency and the cross-sectional area. For a rectangular cross-section the mode cutoff frequencies of both Transverse Electric (TE) and Transverse Magnetic (TM) modes are given by the well-known formula [33]:

$$f_c^{rect} = \frac{c}{2} \sqrt{\left(\frac{n}{a}\right)^2 + \left(\frac{m}{b}\right)^2} \quad (Hz) \quad (22)$$

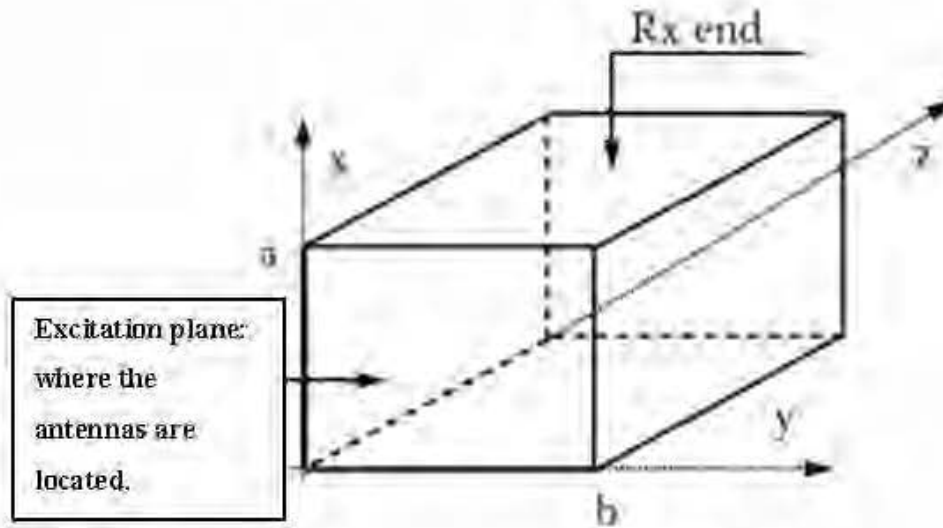


Fig 3.2 Rectangular waveguide.

Where a and b are the width and height respectively. For the TM modes both n and m must be negative. Taking into consideration that the modes are considered to be orthogonal, Exact number of modes can be approximated in an ideal waveguide as follows:

$$N \approx \frac{2\pi ab}{\lambda^2} \quad (23)$$

In particular, for any excitation frequency f , only the modes whose frequencies are higher than the cutoff frequency is excited ($f_c \leq f$). By solving the Maxwell's equations, the field distribution of each mode can be derived in the form of eigenfunctions as follows [34, 35]:

$$E_m^{Rx}(x, y, z) = \sum_{m=1}^{\infty} \sum_{n=1}^{\infty} C_{m,n} E_{m,n}^{eigen}(x, y) \cdot e^{(-\alpha_m + j\beta_m)z} \quad (24)$$

Where α and β are the attenuation coefficient and the phase-shift coefficient, and C_{mn} is the mode intensity at the excitation plane [36].

$$E_{m,n}^{eign}(x, y) \simeq \sin\left(\frac{m\pi}{2a}x + \varphi_x\right) \cdot \cos\left(\frac{n\pi}{2b}y + \varphi_y\right) \quad (25)$$

Where

$$\varphi_y = \begin{cases} 0, & \text{if } n \text{ is odd} \\ \frac{\pi}{2}, & \text{if } n \text{ is even} \end{cases}$$

$$\varphi_x = \begin{cases} 0, & \text{if } m \text{ is odd} \\ \frac{\pi}{2}, & \text{if } m \text{ is even} \end{cases}$$

Arbitrary electromagnetic field inside of such a waveguide can be expanded in terms of the eigenmodes [37, 38]:

$$\mathbf{E}_{x,y,z} = \sum_n \alpha_n \mathbf{e}_n(x, y) e^{-jk_{zn}z} \quad (26)$$

Where $e_n(x, y)$ is the normalized modal function of the electric fields which are represented in (25), and α is the mode amplitudes. It's important to estimate the number of modes in any waveguide environment, obviously for underground mines it's quite complicated especially when high order modes start losing their orthogonality. We can consider calculating the amplitudes of the first modes by knowing the E and H fields in each cross-section of the tunnel. Furthermore, the only modes available in the waveguide are those who can have the same shapes in the existing fields [4], the latter can be obtained by ray tracing model where the mode amplitudes can be obtained by correlating the E field to the mode functions at a certain cross-sectional area Z_R as follows:

$$\alpha = \iint_S \mathbf{E}(x, y, Z_R) \cdot \mathbf{e}_1(x, y) dx dy \quad (27)$$

CHAPTER IV

PERFORMANCE ANALYSIS OF SUITABLE MIMO DOWNLINK SYSTEMS IN UNDERGROUND MINE

4.1 Introduction

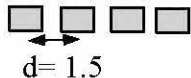
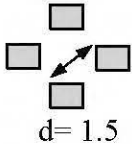
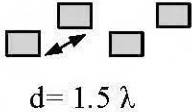
Linear precoding/beamforming systems play a crucial role in the MIMO signal process. For instance, in [40] the authors analyzed the spectral efficiency of a single-cell downlink massive MIMO system with ZF, MRT, and MMSE (minimum mean-square error). In [41], the authors analyzed the performance of the massive downlink MIMO in terms of spectral efficiency, energy efficiency, and link reliability using ZF precoding. The authors in [42] compared the matrix and vector normalization for downlink ZF and MRT precoding and analyzed the ergodic performance of such precoding in a cell-boundary users scenario. Although the above works offer sensible results concerning the performances of the linear precoding schemes, they lack the comparison of ZF and MRT performances in terms of the correlation factor that occurs in confined environments. However, according to recent studies which showed that beamforming didn't perform well in narrow tunnels, the aim of this section is to demonstrate that for MIMO system with small antenna array size, and for a suitable precoding technique at the transmitter and receiver, beamforming can perform better in terms of ergodic capacity compared to none precoding scheme.

In this chapter, we will analyze and compare the performances of MRT and ZF in underground mine tunnels environment. Thus, we will disregard using MMSE as it didn't perform well compared to MRT and ZF environments and that according to Karatza [5]. Additionally, for a narrow tunnel, we tested three different antenna configurations in order to obtain the suitable alignment. Simulations are done for both schemes concerning data rate, transmit power and SINR. The various results are analyzed in order to compare the performance of the techniques in the mine environment.

4.2 MIMO Antenna Alignment

The aim of this section is to obtain an optimal antenna configuration in mine tunnels. Therefore, we consider taking three antenna alignments: perpendicular to the tunnel axis, circular, and zigzag as shown in table I. The reason behind taking these alignments is that according to the recent studies in [40] and [41]. The perpendicular alignment is considered to give the lowest correlation between the antennas and correspondingly the highest capacity can be obtained. However, for a 4-element antenna array, a circular array with a certain angle between the normal and the longitudinal direction is better

TABLE I. ANTENNA ALIGNMENTS

Antenna Alignment		
<i>Perpendicular</i>	<i>Circular</i>	<i>Zigzag</i>
 $d = 1.5$	 $d = 1.5$	 $d = 1.5 \lambda$

than a linear array alignment and that for an LTE study done in a railway [42]. Likewise, a study done in [43] showed that zigzag alignment in Microcell (LOS), small microcell (NLOS), and indoor gave an acceptable result too. Thus, for this reason, we will evaluate those alignments in the underground mine environment.

4.3 System Model:

Wireless InSite's ray tracing capability has been used to set up a small underground old gold mine scenario located in Val d'Or, Canada. The tunnel is imported as a CAD file. The imported mine's walls have some protrusions as shown in Fig 4.1.B. The tunnel stretches over a length about 400 m and it's broken down into two parts with 200 m length each: a LOS part and a NLOS part as shown in Fig 4.1.A. A virtual array of 4 elements is used at both sides at the link. The transmitting and receiving antennas used are dipoles which are vertically polarized and uses a wide raised-cosine pulse. Correspondingly, a 2λ separation distance must be taken between antennas to ensure decorrelation between the subchannels. Indeed, a larger separation will not necessarily work for this distance. In contrast, smaller separation will increase the correlation, a further explanation can be found in [29]. The carrier frequency used is 900 MHz, 2.4 GHz and 5.8 GHz. In Fig 4.1, we placed the transmitter array at point A, and the receiver points are aligned along the trajectory from point A to B with a 1-meter separation distance. According to the previous experimental work in [29] and [30], it has been proved that aligning the antenna array perpendicular to the tunnel axis will perform better than other orientations. Hence, we adopt this orientation in our study. The dielectric constant used in the walls is different from that in the ceiling and the floor which is 5.7 for the walls and 5.1 for the ceiling and floor. Besides, we considered that the CSI is known to the receiver. The configuration of ray tracing calculation is defined to use wireless InSite's GPU accelerated X3D ray model, the model can handle arbitrary geometry and transmitters/receivers at any height, this accurate model includes

reflections, transmissions and diffractions along with frequency dependent atmospheric absorption. Besides, ray tracing defined to include propagation paths with up to six reflections and one diffraction omitting transmissions to limit calculation to the outdoors.

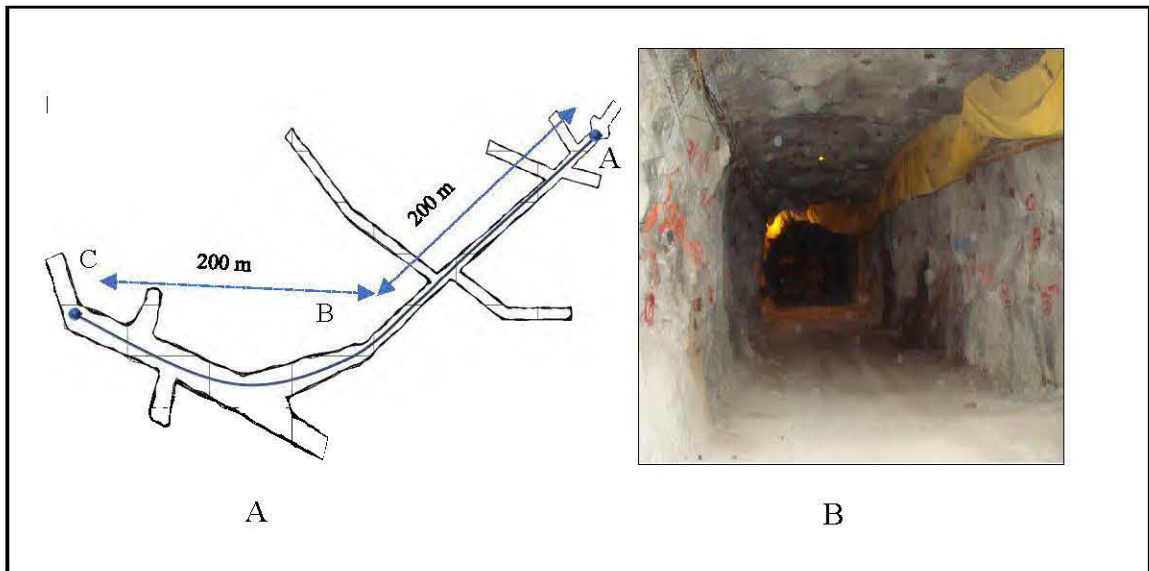


Fig.4.1: (A) CANMET schematic and (B) CANMET mine image.

4.4 Theoretical Results:

4.4.1 Diversity Techniques Results Discussion:

Cumulative density function versus capacity and capacity versus distance was calculated for the systems supporting ZF and MRT, for the 900 MHz which is represented in Fig. 4.2 and Fig. 4.3. Fig. 4.4 represents the CDF of the highest capacities among the six diversity methods for the 2.4 GHz and the 5.8 GHz frequencies. Thus, we can observe that using MRT precoding at the transmitter with MRC receiving diversity can give an optimal performance compared to the other combinations for the three frequencies. Besides, in Fig. 4.4 we can observe that for higher frequencies the

capacity will increase with a 10 bits/sec/Hz difference compared to the 900 MHz. However, MRT/EGC performed well in the three scenarios but still didn't exceed the MRT/MRC capacity in three scenarios. Hence, we can interpret that MRT/MRC configuration defines a low correlated channel whereas the NB/EGC configuration defines a high-correlated channel. Fig.4.5 shows the SINR versus distance. We can realize that MRT/MRC and PC/EGC configurations performed well, and they are quite close to the MRT/SC. On the contrary, the NB/MRC and NB/EGC records the lowest SINR. Indeed, we can realize that the attenuation rate for techniques with precoding is much lower than other techniques. This illustrates the well-known conclusion that the presence of spatial correlation in MIMO channels leads to significant performance degradation for the spatial multiplexing scheme. It's relevant hence in Fig.4.6 and in Fig.4.7 which presents the total received power versus distance, the total power received by the non-precoding schemes where much lower than the other schemes particularly in the far field region, while in our case this region is after 100 m, where the correlation between the channel matrix is high enough, which is expected to be higher than 0.8 at any point.

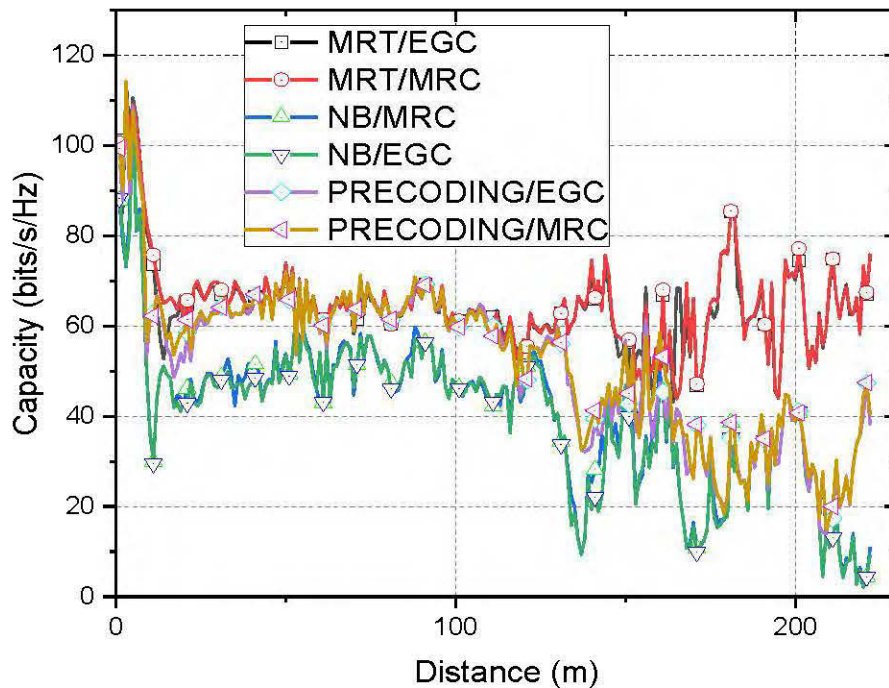


Fig. 4.2: Capacity for different MIMO schemes for the 900 MHz.

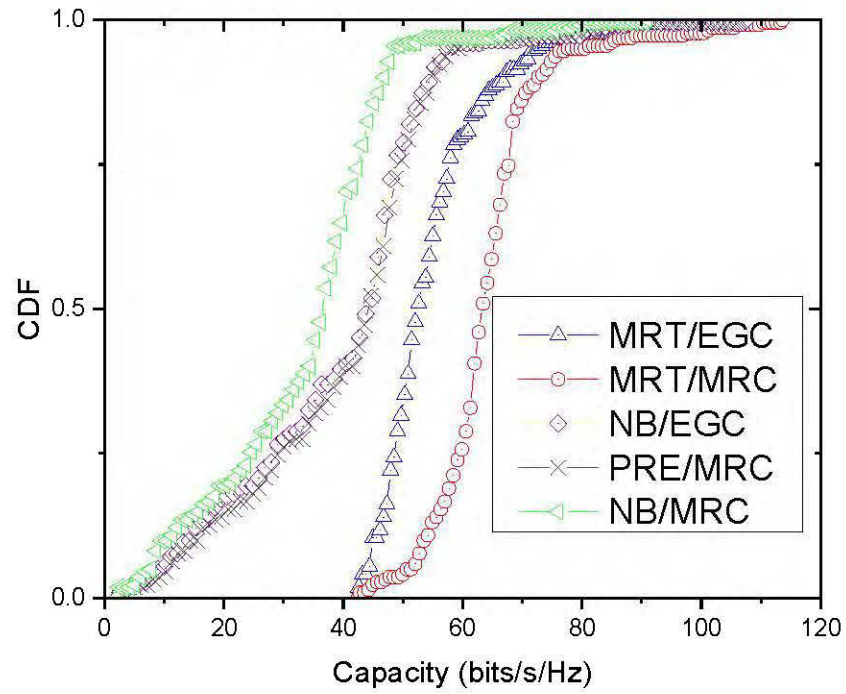


Fig.4.3: Capacity for different MIMO schemes in CDF form for the 900 MHz.

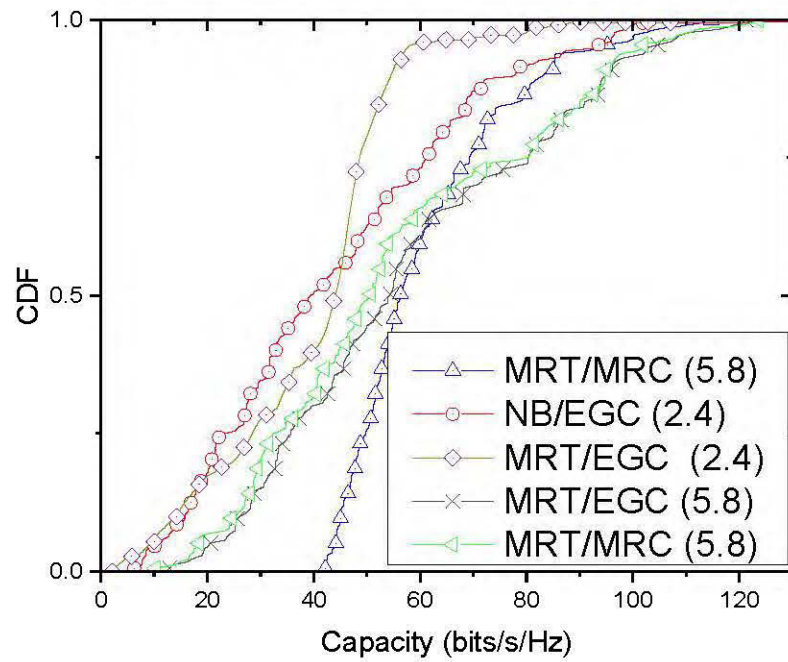


Fig.4.4: Capacity for different MIMO schemes in CDF form for 2.4 GHz and 5.8 GHz.

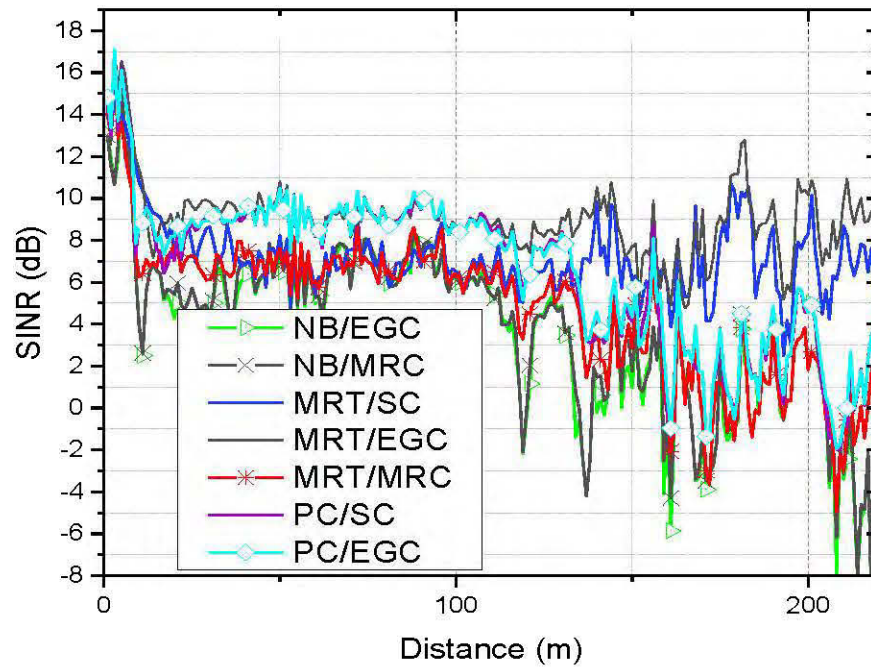


Fig.4.5: SINR vs Distance between different MIMO systems for 900 MHz.

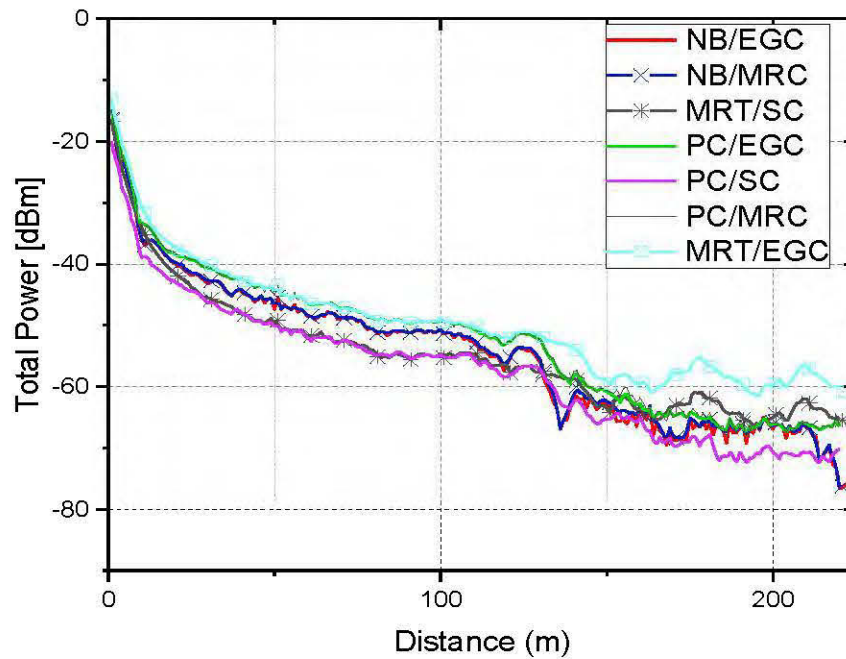


Fig. 4.6: Power versus distance between different MIMO systems for 900 MHz

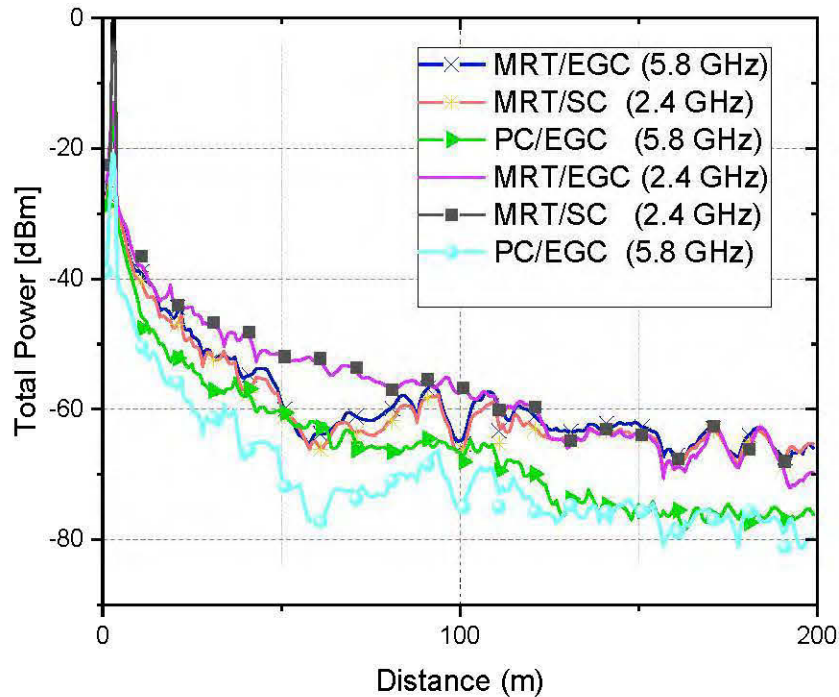


Fig. 4.7: Power versus distance between different MIMO systems for 2.4 GHz and 5.8 GHz.

4.4.2 MIMO Antenna Alignments Results Discussion:

In this section, we used the same environment and the same measurement procedure as in section 4.3, except that the simulation now is done in the NLOS part from point B to point C in Fig.4.1. In addition, we considered taking 2×2 , 4×4 and 6×6 MIMO antenna arrays. The results obtained in Fig.4.8 which is for the 900 MHz shows that the zigzag alignment has unfavorable power loss compared to the two other alignments. Moreover, we can see that the circular alignment performed better than the perpendicular one. In addition, we can realize the fast fluctuation in the near field region where the propagation of EH modes is more like the propagation in a free space environment. Besides, we can analyze that the breakpoint appears to happen after the tunnels curve with the propagation of the lowest modes where we can obtain that 4×4 MIMO systems perform nearly the same as the 6×6 MIMO systems. In Fig. 4.9, we chose the highest

three total power for the 2.4 GHz and 5.8 GHz. We can realize a power drop around 10 dBm to 15 dBm as frequency increases. Where in the 2.4 GHz and 5.8 GHz, 4×4 circular still records the highest power. In Fig. 4.10 and Fig. 4.11 we can analyze that 4×4 circular configuration records the highest capacity in the far-field region for the three frequencies, while SISO and 6×6 circular alignment scores the lowest capacity, the reason behind this low capacity of the 6×6 circular alignment is that it's not possible to place 6 antennas circularly with a 1.5λ space between the antennas. For this reason, a correlation occurs between the transmitted signals and leads to this capacity drop. So, it's better to avoid using the latter alignment with 6 antennas in any environment.

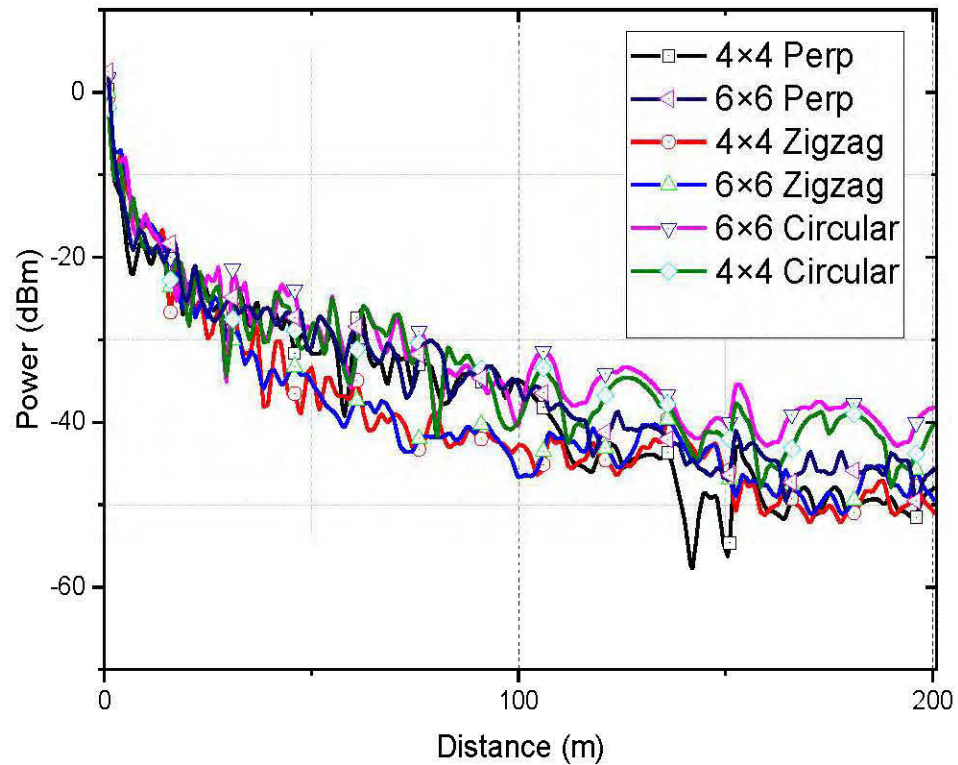


Fig. 4.8: Power versus distance plot in the NLOS part for 900 MHz.

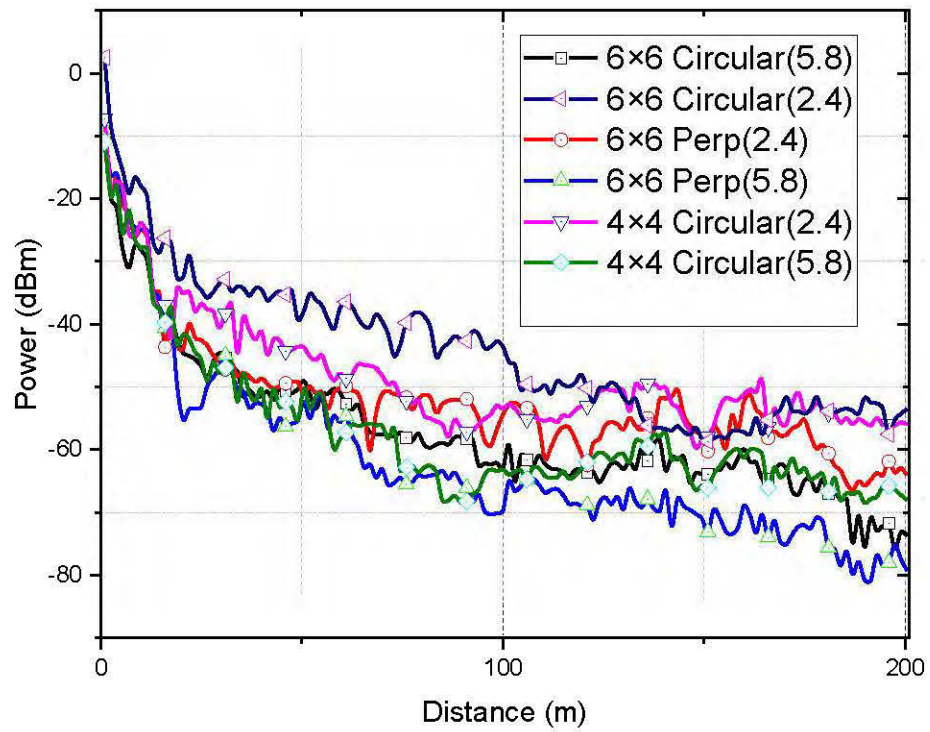


Fig. 4.9: Power versus distance plot in the NLOS part for 2.4 GHz and 5.8 GHz

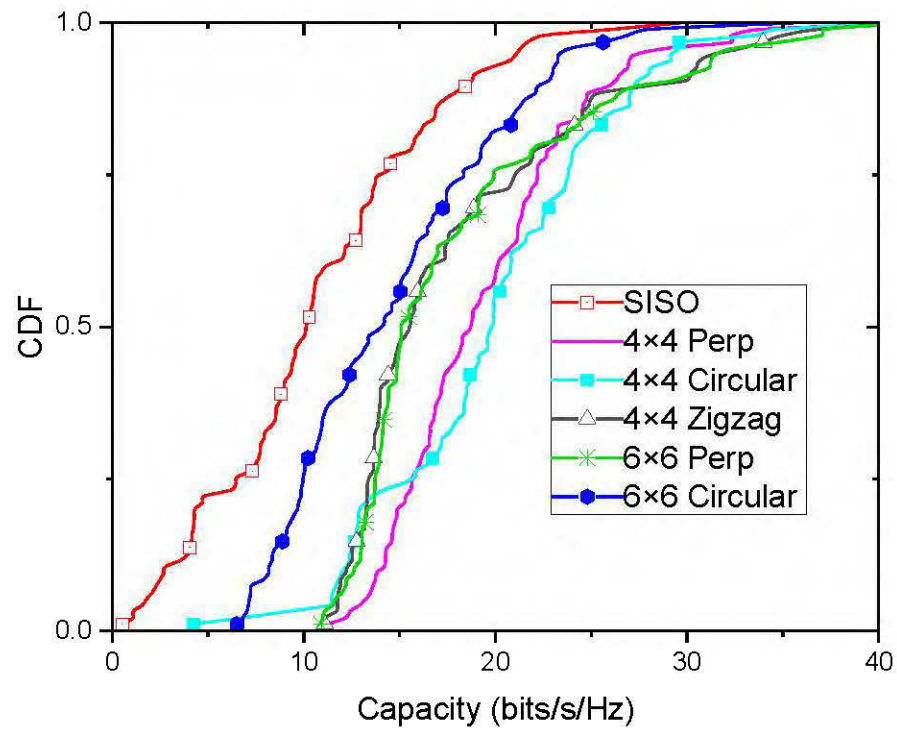


Fig. 4.10: Capacity of different MIMO antenna alignments for the 900 MHz.

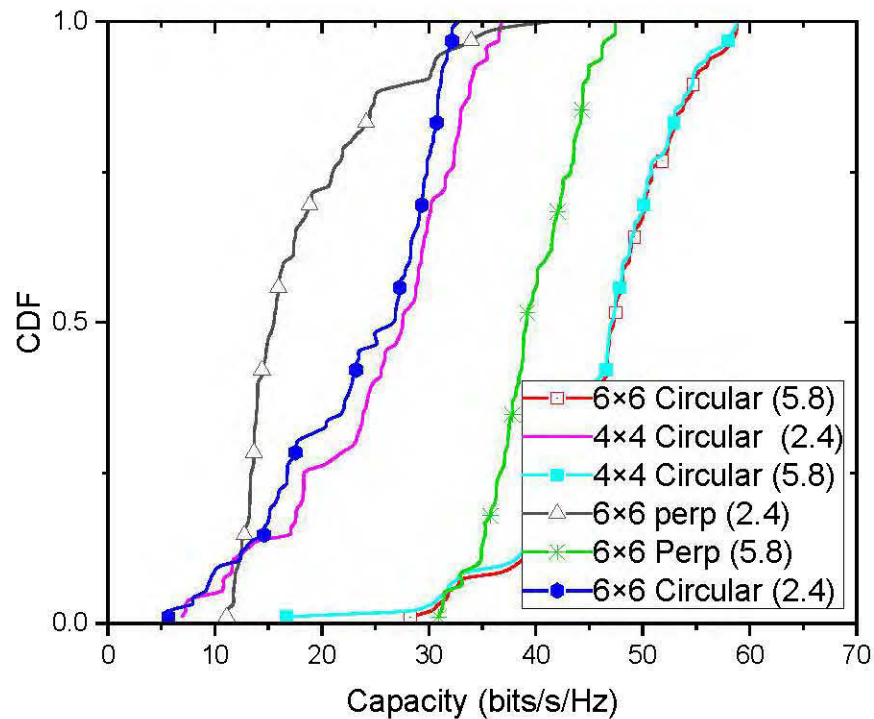


Fig. 4.11: Capacity of different MIMO antenna alignments for the 2.4 GHz and 5.8 GHz.

4.5 Conclusion

We can realize from these simulations that precoding can be effective in mine tunnels especially if we used MRT/MRC and MRT/EGC combinations at both the transmitter and receiver. The usage of the three different frequencies supports this conclusion. Contrarily, without beamforming, we will have a poor performance even if we have a high SNR. This illustrates the well-known conclusion that the presence of spatial correlation in MIMO channels leads to significant performance degradation for the spatial multiplexing scheme. Besides, perpendicular alignment didn't perform as it was expected in the mine environment, where having Circular alignment can overcome the perpendicular in both, the power delivered and capacity.

CHAPTER V

ANALYSIS OF MIMO CHANNEL CHARACTERISTICS IN LOSSY
WAVEGUIDES

5.1 Introduction

In this chapter, we have conducted theoretical MIMO analysis in underground mines to interpret the effect of increasing antenna array elements on the system's capacity. The study is based on theoretical results where we consider that mines can act as tunnels in case of comparing them to oversized dielectric waveguide where many modes can propagate. In addition, we derived an approximation formula that can be used to calculate the number of modes in a straight and curved mine tunnel. Wherein this study we used the empirical model to estimate the number of modes in a rectangular cross-section mine.

5.2 Theoretical Approach

5.2.1 MIMO Capacity

If we consider taking $M \times N$ memoryless MIMO system, the maximum capacity without water-filling and in the presence of white Gaussian noise is given by Foschini et al.

$$C = \log_2 \det(\mathbf{I}_m + \sigma \cdot \mathbf{H}\mathbf{H}^H) \text{ bits/s/Hz} \quad (28)$$

The channel capacity can be expressed in terms of the singular values of the matrix as follows:

$$C = \sum \log_2 \left(1 + \frac{E_x}{\sigma^2} \lambda_i \right) \quad (29)$$

For $H = I$, and for identical number of antennas at the transmitter and receiver N , we can represent MIMO capacity in (29) where the maximum capacity is achieved for independent subchannels as follows [31]:

$$C = N \det(1 + \sigma) \quad (30)$$

From these equations, we can interpret that improving the system's capacity will undoubtedly depend on the number of antennas and the SNR. Hence, we assumed taking a constant SNR, thus we used Euclidean norm to normalize the complex H matrix. When constant SNR is assumed, it allows emphasizing the effect of channel change on the correlation and thus the change in path loss with distance is removed.

5.2.2 Performance Reduction Factors in Tunnels

As we mentioned that in tunnel mines, we have a poor scattering environment and the channels may be correlated due to the confined environment in contrast with the free space. In Fig. 5.1 we can interpret from the graph that angular spread in tunnel is small, which causes increasing the correlation between the arrays. Furthermore, for channel correlation, we have three factors which affect the ergodic capacity of the system which depends on:

- cross-section of the tunnel
- coupling between excited modes at the transmitter
- coupling between modes in the waveguide due to losses and surface roughness

- coupling between modes at the receiver.

The coupling between excited modes at the transmitter may have a negligible effect on the performance at the far field region, considering only the continuation of the fundamental modes. Indeed, according to study in [7] where they calculated the correlation between modes at different antenna separations in a subway metro. The correlation between the modes excited by antennas j_1 and j_2 can be demonstrated in equations (31) and (32) where the results conducted shows that the propagation in the narrow width tunnel results in a high correlation between modes compared to a wider tunnel. Indeed, the correlation between modes increases with respect to the distance but obviously, it will not have drastic effects on the capacity since we end up with a limited number of modes at the receiver.

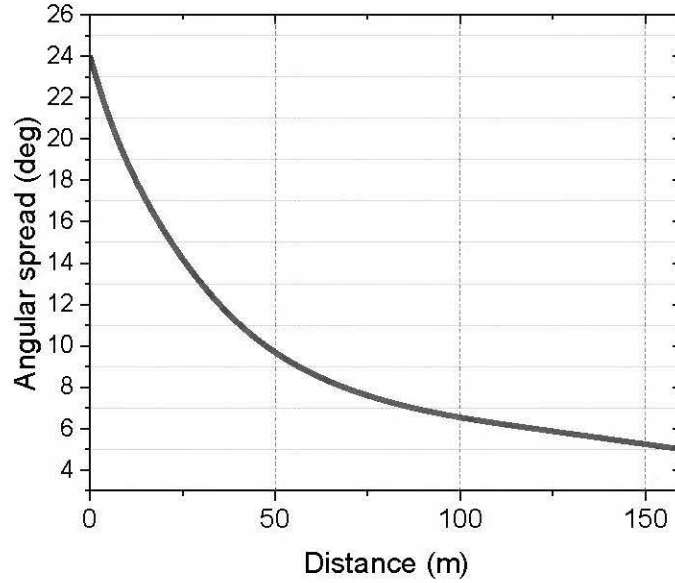


Fig. 5.1: Angular spread vs distance in CANMET

$$\rho_{j_1 j_2}^{\alpha}(z) = \frac{|\phi_{\alpha}(j_1, j_2)|}{|\phi_{\alpha}(j_1, j_1)\phi_{\alpha}(j_2, j_2)|^{1/2}} \quad (31)$$

$$\phi_{\alpha}(j_1, j_2) = \frac{1}{MN} \sum_m \sum_n (\alpha_{m,n}(z, j_1) - \langle \alpha_{m,n}(z, j_1) \rangle) \times (\alpha_{m,n}^*(z, j_2) - \langle \alpha_{m,n}^*(z, j_2) \rangle) \quad (32)$$

Where ϕ_{α} is given by the estimate and $\langle \cdot \rangle$ denotes the expectation over the modes [3]. Moreover, the performance of the MIMO systems in tunnels is mainly affected by many factors like the tunnel size, antenna position, antenna polarization, and the MIMO antenna array size which is our main focus, these factors with the rank reduction of the transfer matrix reduces the capacity of the wireless system.

5.2.3 Degenerated Channels

Low capacity can occur in MIMO even when we have zero correlation between the signals. This is the case of degenerated channels. For MIMO, the wireless channel can be represented as a matrix of the fading channels with additive noise.

$$\bar{y} = H\bar{x} + \bar{w} \quad (33)$$

Where y is the received signal array, x is the transmitted signal and w is the additive white Gaussian noise. From Foschini et al MIMO capacity formula [32], we can obviously realize that the channel capacity depends on the channel matrix H . Furthermore, H can be represented by the SVD as:

$$H = U\Sigma V^H \quad (34)$$

Replacing H in (34), we can represent the system as

$$\bar{y} = U\Sigma V^H \bar{x} + \bar{w} \quad (35)$$

By Performing precoding at the transmitter, we will have:

$$\tilde{y} = \Sigma \tilde{x} + \tilde{w} \quad (36)$$

(36) can be demonstrated as t parallel channels, furthermore t degrees of freedom:

$$\begin{aligned} y_1 &= \sigma_1 \tilde{x}_1 + \tilde{w}_1 \\ y_2 &= \sigma_2 \tilde{x}_2 + \tilde{w}_2 \\ &\vdots \\ y_t &= \sigma_t \tilde{x}_t + \tilde{w}_t \end{aligned} \quad (37)$$

In (37) the H matrix is decomposed into a t parallel channels where spatial multiplexing can be applied. Indeed, as was proposed by Loyka, that individual waveguide modes can act as MIMO propagation channels [32], now the orthogonal modes can propagate through these channels. In an ideal waveguide, the modes are considered orthogonal if the mode coupling factor is expressed in the following equation [loyka]:

$$\iint e_n e_m \, dx dy = \delta_{mn} \quad (38)$$

$$\text{Where} \quad \begin{cases} \delta_{mn} = 1 & \text{if } m = n \\ \delta_{mn} = 0 & \text{otherwise} \end{cases} \quad (39)$$

Where $e_n(x, y)$ is the normalized modal functions of the electric field.

For mine tunnel environment, the orthogonality is still applied for the first 60 mods, where the mode coupling factor is considered to be neglected [33]. Furthermore, high order modes are subjected to high attenuation at large distances, which in terms decrease the number of actual modes that contributes to the total power at the receiver. Accordingly, spatial multiplexing can be applied. Consequently, if we have an $M \times N$

MIMO system we must have $L \geq \min(M, N)$ to profit from this technique. Where L is the number of active modes [8], [30].

5.3 System Model and Theoretical Validation

5.3.1 Effects of Changing Dimensions of the Tunnel Results:

In this section, we used the same environment and the same measurement procedure as in section 4.3, except that the simulation now is done from point A to point C as its shown in Fig. 5.2. Also, we set up two scenarios, which have the same height and length (H : 3.5 m, L : 400 m) but with different width (w_1 : 3.5 m, w_2 : 7 m) and named as Case I and Case II.

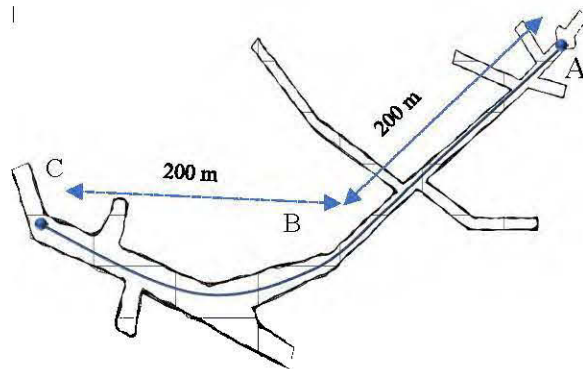


Fig. 5.2: CANMET schematic.

In Fig. 5.3, Fig. 5.4 and Fig. 5.5 we can interpret from the graphs that the wider tunnel records a higher number of modes within the first 200 m, and that's because in this region the tunnel's act as a free space environment where the lower angular spread in the narrowest tunnel causes a higher correlation between the arrays, which in terms causes deterioration in the received power. Contrarily, the coupling between excited modes at the transmitter may have a negligible effect on the performance in the far field region. Correspondingly, we can see that after 300 m, the two tunnels record nearly the same number of modes.

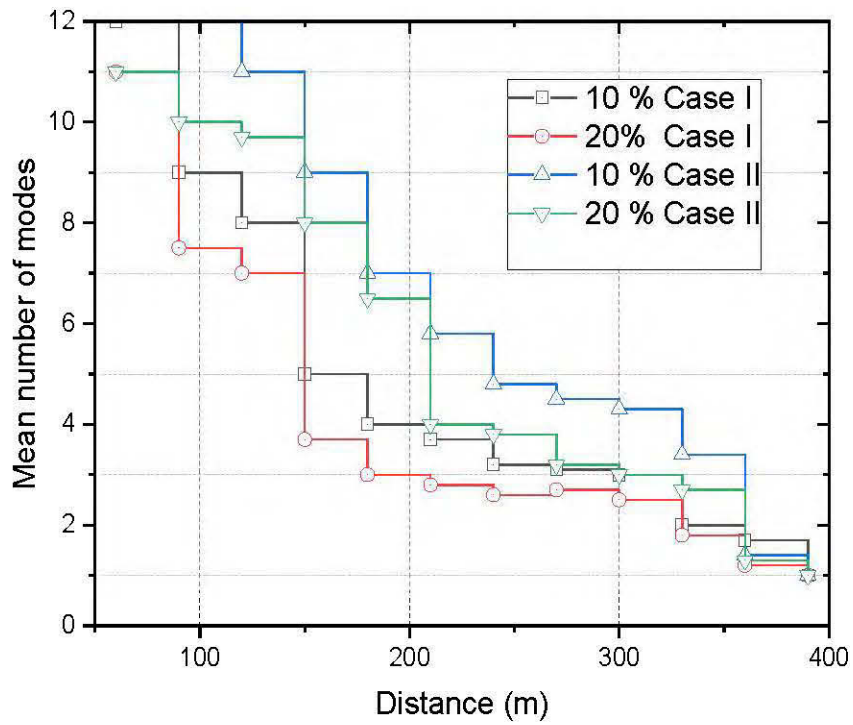


Fig. 5.3: Mean number of modes in CANMET for Case I and Case II (900 Mhz).

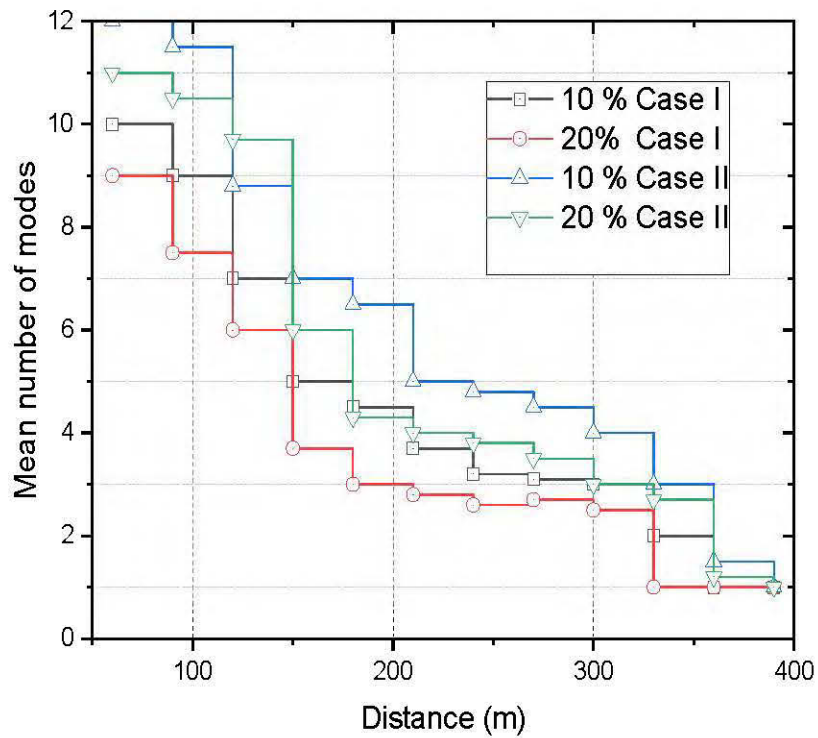


Fig. 5.4: Mean number of modes in CANMET for Case I and Case II (2.4 GHz).

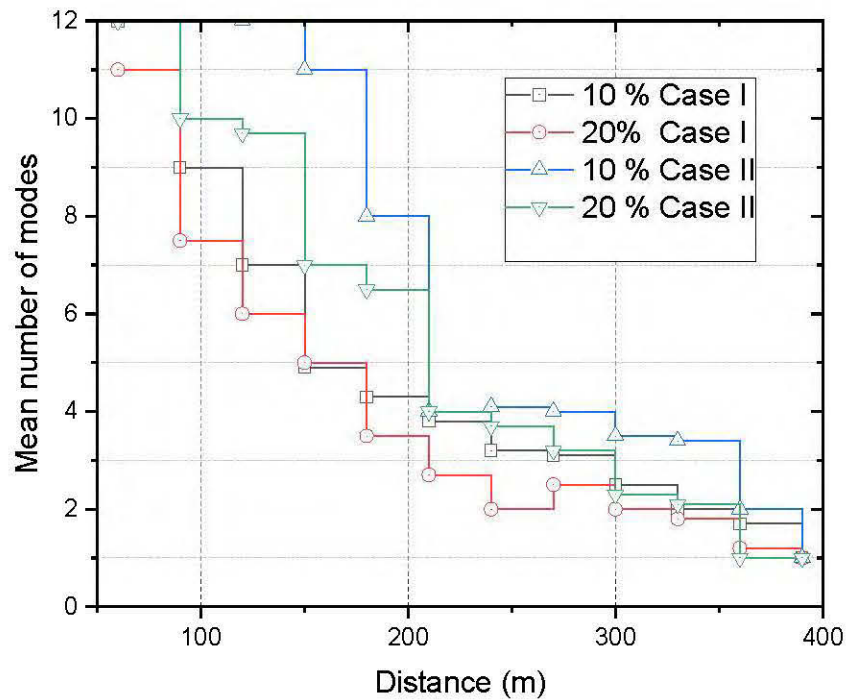


Fig. 5.5: Mean number of modes in CANMET for Case I and Case II (5.8 GHz).

5.3.2 Effects of Increasing Antennas on Capacity and Power Results:

The environment and measurement procedures used here are the same as in the previous section, except that we used Case I measurements. In addition, we considered taking 2×2 , 4×4 and 6×6 MIMO antenna arrays to examine the power and capacity of each system. As shown in Fig. 5.6 and Fig. 5.7. In the near field region, the signal drops fast and we can analyze a big fluctuation wherein the far field region the fundamental modes now form 90% of the total power, obviously we can analyze a drop in the attenuation rate in the NLOS, the breakpoint can be analyzed visually after 130 m and that by analyzing a periodic signal. We can analyze that the performance of high orders MIMO are not as we can expect in the free space, because the fundamental modes which are orthogonal to each other are smaller than the propagation channels. Furthermore, if we consider taking higher frequencies, we expect to have a less attenuation drop but we don't expect improvement in the capacity with increasing the number of antennas.

In Fig. 5.8 and Fig. 5.9, we can analyze that the capacity of 2×2 and 4×4 MIMO systems are nearly the same and in sometimes they exceed the capacity of the 6×6 MIMO system, and this is the situation where the degrees of freedom of the system is reduced with distance and it became less than the available transmitting channels. We can expect that 6×6 MIMO can perform better in Case II tunnel compared to 4×4 MIMO. In brief, if we have M×N MIMO system we must have $L \geq \min(M, N)$ to profit from this technique. Where L is the number of active modes [8] [30].

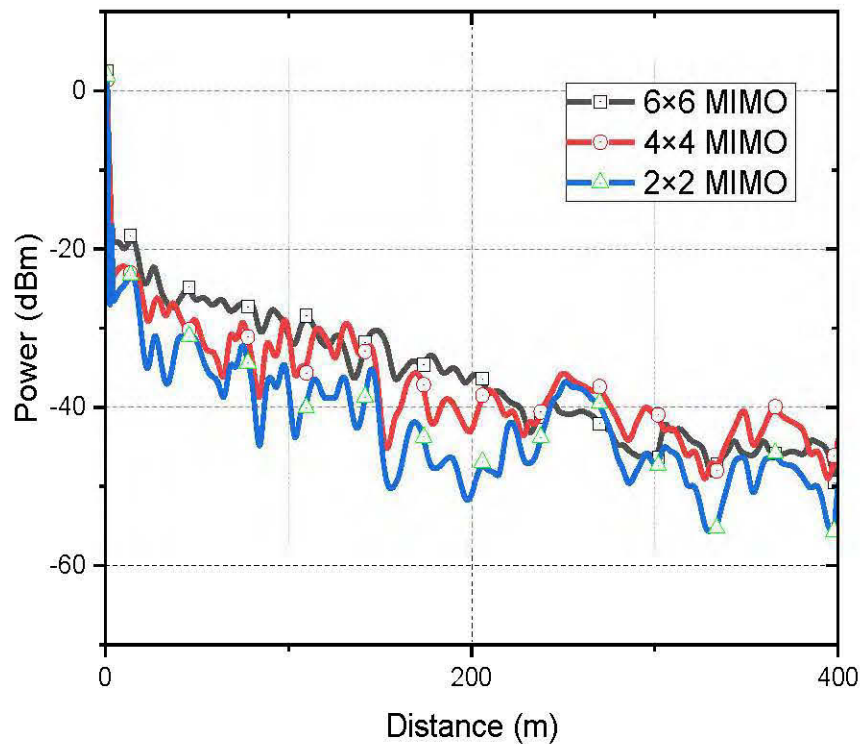


Fig. 5.6: Power versus distance between different MIMO systems (900 MHz).

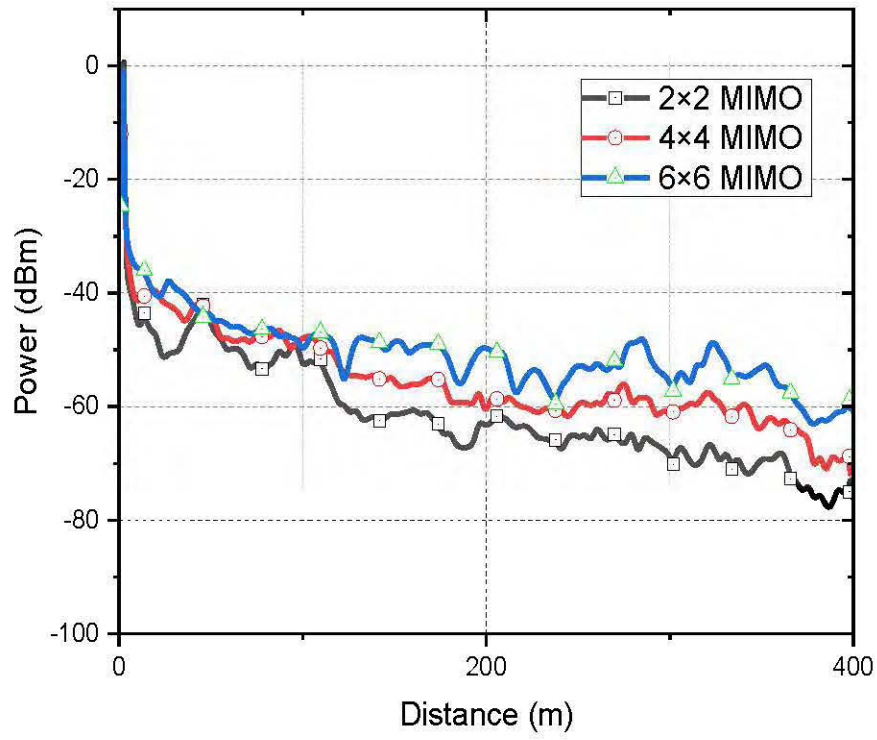


Fig. 5.7: Power versus distance between different MIMO systems (5.8 GHz).

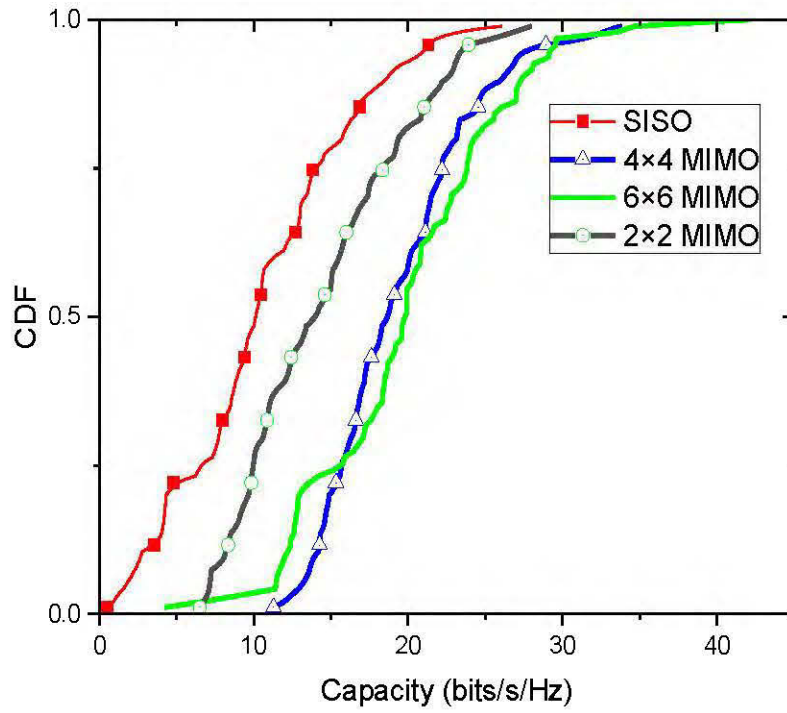


Fig. 5.8: CDF of different MIMO systems (900 MHz).

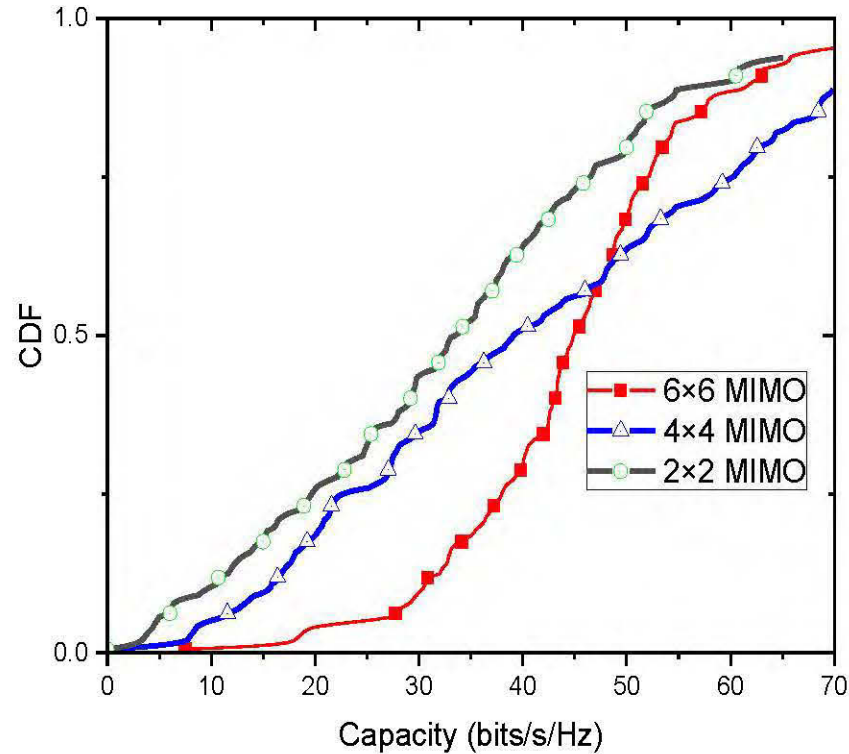


Fig. 5.9: CDF of different MIMO systems (5.8 GHz).

5.4 Estimating the Number of Modes in Underground Mine Tunnel:

5.4.1 Simulation Setup:

In this section, we will use ray tracing at straight and curved shape tunnels to evaluate the number of modes. The calculations are made at a various collection of simulated tunnels which their length and height vary from 3 to 6 meters. The tunnels stretch over a length about 1000 m. The frequency band considered in this study is taken from 900 MHz to 1.5 GHz. We numerically computed the number of TE and TM active modes which represents 10% of the received power in the lossy tunnel as a function of normalized frequency for the first 100 modes. We then carried out a regression analysis

to find the best nonlinear symmetrical sigmoidal equation that fit these data. where the obtained equation can take values only within the simulated range.

5.4.2 Straight Tunnel

For the straight tunnel, the transmitting and receiving antennas used are vertically polarized dipoles that are perpendicular to the tunnel's axis. In order to calculate the number of modes. A modematching technique is used, Once the mode intensity is determined in the excitation plane, the mode propagation is mostly governed by the tunnel itself. Then the EM field in the rest of the tunnel can be predicted by summing the EM field of each mode [2]. The obtained equation is as follows:

$$N = \frac{\pi}{\lambda^2} (0.6 \times A^{0.21}) \left(-0.26 + \frac{1.26}{1 + \left(\frac{L}{5.15}\right)^{2.18}} \right) \quad (40)$$

Where L is the distance from the transmitter and A is the cross-sectional area, this equation depends on cross-sectional area, frequency, and distance from transmitter.

5.4.3 H-bend Tunnel

This section explores the impact of curved subway tunnel on the MIMO channel which can affect the number of modes. Correspondingly, the main aim is to highlight the effects of curved tunnels on the number of propagating modes. In this work, we are limited to one arc shape. which exists predominately in every mine which is the h-bend shape. The scenario is provided in Fig.5.10. We had set the antenna array in 3 positions to see the effect of the curvature on the channel impulse response. The uniform linear antenna arrays are perpendicular to the centerline except for the ones in the curved part they are parallel to the radius direction of the arc. The obtained formula for the curved tunnel is as follows:

$$N = \frac{\pi}{\lambda^2} (0.6 \times A^{0.21}) \left(-1.26 + \frac{26.16}{1 + \left(\frac{L}{363.4} \right)^{1.71}} \right) \quad (41)$$

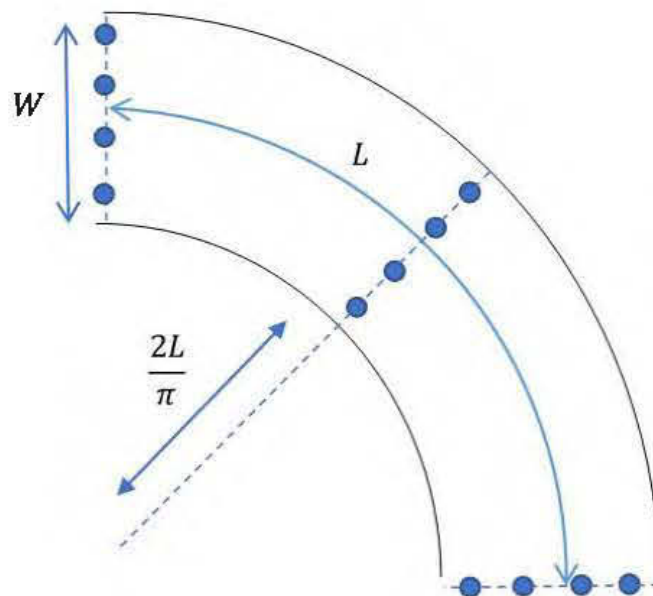


Fig. 5.10: Curved tunnel scheme.

5.5 Results Discussion:

As shown in Fig. 5.11, the estimation formula gave acceptable results compared to the theoretical values for a simulated mine tunnel with width and height of 3 meters, and frequency of 900 MHz in the two scenarios, noting that the estimated values represent the active modes with 10 % contribution to the total received power. Furthermore, decreasing this percentage will lead to a less accurate prediction. Noting that an active channel must have at least 10 % contribution to the received signal.

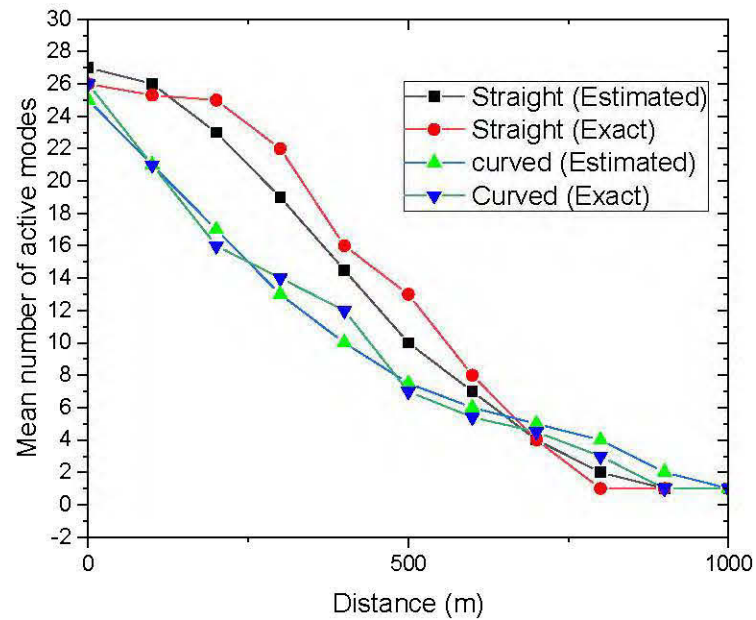


Fig. 5.11: Estimated vs exact number of modes at a mine with 3 meters width and height, and a frequency of 900 MHz in curved and straight tunnels

5.6 Conclusion:

In this chapter, we obtained that in order to profit from the spatial multiplexing of the MIMO system, we must have a number of antenna arrays which is equivalent to the number of active modes at the receiver. Besides we used empirical approach to obtain equation which estimates the number of modes in a straight and curved mine. Applying the previous techniques can facilitate the employment of MIMO system in the mine and save complexity.

CHAPTER VI

CONCLUSION

In this work, we have reached our objectives and thereby contributed to the efficient and effective deployment of MIMO-based wireless systems in underground gold mine environment.

6.1 Contributions

By the theoretical studies, we have contributed that Beamforming can be effective in mine and drop using it will reduce the performance of the MIMO system. The best combination of precoding systems which record the highest capacity was the MRT/MRC and MRT/EGC. By embracing these systems, we can augment the capacity by 5 to 10 %. This percentage can diversify depending on the tunnel cross-sectional dimension and the antenna configuration. In chapter 4, a theoretical study was conducted in an underground mine tunnel model in order to demonstrate the relation between capacity and number of propagating channels. A channel model which can calculate the EM field in the near and far field region is used to prove that in order to profit from the spatial multiplexing of the MIMO system we must have a number of antenna arrays which is equivalent to the number of modes at the receiver. Otherwise, MIMO improvement will be limited. In addition, implementing circular configuration with a 1.5λ separation distance between the antenna can enhance the performance of the system by reducing the correlation and increasing the capacity while the most used ULA configurations show limited performance. Furthermore, estimating the number of antennas in the provided tunnel shapes can be beneficial by saving time and cost to

engineers, where the equation gave an acceptable result in the straight and curved mine tunnels.

6.2 Future work

The next step will be to attempt a follow-on investigation of wave propagation in the vicinity of more intricate geometries such as curves and junctions. Besides, for the estimating part, we only considered taking one curved scenario and a basic straight tunnel. Consequently, obtaining an estimation formula that considers different shapes can be more practical and realistic. Indeed, it would be beneficial to determine whether it is necessary to include surface roughness in the estimated equations and if that can drastically change the orthogonality between the modes in the tunnel.

APPENDIX A

NARROW BAND ASSUMPTION IN WIRELESS CHANNEL MODELING

Due to MPE, Channel fading coefficient can be represented as:

$$h(t) = \sum_{i=0}^{L-1} a_i \delta(t - \tau_i)$$

The transmitted signal can be represented as:

$$S_p(t) = \text{Re} \{ s(t) e^{j2\pi F_c t} \}$$

$S(t)$: Complex baseband signal

F_c : Carrier frequency

The received signal can be represented as:

$$\begin{aligned} y_p(t) &= \sum_{i=0}^{L-1} \text{Re} \{ a_i S(t - \tau_i) e^{j2\pi F_c (t - \tau_i)} \} \\ &= \sum_{i=0}^{L-1} \text{Re} \{ (a_i S(t - \tau_i) e^{-j2\pi F_c \tau_i}) e^{j2\pi F_c t} \} \\ &= \text{Re} \{ \sum_{i=0}^{L-1} (a_i S(t - \tau_i) e^{-j2\pi F_c \tau_i}) e^{j2\pi F_c t} \} \\ y(t) &= \sum_{i=0}^{L-1} a_i S(t - \tau_i) e^{-j2\pi F_c \tau_i} = 0 \end{aligned}$$

Assuming narrow band and that's because $F_c \ll F_m$: $(s(t) - \tau_i) \cong s(t)$

Where F_m is the message frequency.

Accordingly:

$$\begin{aligned} y(t) &= \left(\sum_{i=0}^{L-1} a_i e^{-j2\pi F_c \tau_i} \right) s(t) \\ y(t) &= h S(t) \end{aligned}$$

REFERNECES

- [1] Caire, G., and S. Shamai. "On the Capacity of Some Channels with Channel State Information." Paper presented at the Proceedings. 1998 IEEE International Symposium on Information Theory (Cat. No.98CH36252), 16-21 Aug. 1998 1998.
- [2] Deotale, N., U. Kolekar, and V. Hendre. "Ergodic Capacity Based Antenna Selection in Mimo for Rayleigh Fading." Paper presented at the 2015 International Conference on Information Processing (ICIP), 16-19 Dec. 2015 2015.
- [3] Ding, B., X. Chen, X. Zhang, Y. Zhang, and R. Yan. "Svd-Based Dictionary Learning for Bearing Fault Diagnosis." Paper presented at the 2016 International Symposium on Flexible Automation (ISFA), 1-3 Aug. 2016 2016.
- [4] Hrovat, Andrej, Gorazd Kandus, and Tomaz Javornik. "A Survey of Radio Propagation Modeling for Tunnels." *IEEE Communications Surveys & Tutorials* (09/17 2013).
- [5] Karatza, Georgia, K. Peppas, and Nikos Sagias. "Effective Capacity of Multi-Source Multi-Destination Cooperative Systems under Co-Channel Interference." *IEEE Transactions on Vehicular Technology* PP (06/15 2018).
- [6] "Rock Solid: The Mining Industry in British Columbia 2008," Price Waterhouse Coopers LLP,Vancouver, BC, 5 May 2009.
- [7] P. Delogne, "Mini-review: EM propagation in tunnels," *IEEE Trans. Antennas Propag.*, vol. 39, pp.401-406, 1991.
- [8] W. C. Jakes, *Microwave Mobile Communications*, New York: McGraw-Hill, pp.110, 1974, p. 110.2012.
- [9] A. H. Wong, M. J. Neve, and K. W. Sowerby, "Antenna selection and deployment strategies for indoor wireless communication systems," *IET Commun.*, vol.4, pp. 732-738, 2007.
- [10] C. Hermosilla, R. Feick, R. Valenzuela, and L. Ahumada, "Improving MIMO capacity with directive antennas for outdoor-indoor scenarios," *IEEE Trans. Wireless Commun.*, vol. 8, pp. 2177-2181, 2009.
- [11] Molina-Garcia-Pardo, M. Lienard, P. Degauque, D.G. Dudley, and L. Juan-Llacer, "Interpretation of MIMO channel characteristics in rectangular tunnels from modal theory," *IEEE Trans. Veh. Technol.*, vol. 57, pp. 1974-1979, 2008.
- [12] S. Loyka, "Multiantenna capacities of waveguide and cavity channels," in *CCECE 2003 – Canadian Conference on Electrical and Computer Engineering. Toward a Caring and Humane Technology* (Cat.No.03CH37436), 2003.

- [13] E. C. Robert, "Basic Electromagnetic Theory," in *Field Theory of Guided Waves*, ed: IEEE, 1991.
- [14] J. Foschini and M. Gans "On the limit of wireless communications in a fading environment when using multiple antennas," *Wireless Personal Commun.*, vol. 6, pp. 311-335, 1998.
- [15] A. Paulraj, R. Nabar, and D. Gore, "Space-Time Propagation," *Introduction to Space Time Wireless Communications*, Cambridge: University Press, 2003.
- [16] A. Emslie, R. Lagace, and P. Strong, "Theory of the propagation of UHF radio waves in coal mine tunnels," *IEEE Trans. Antennas Propag.*, vol. 23, pp. 192-205, 1975.
- [17] Bonek, E. . MIMO propagation channel modeling. 7th European Conference on Antennas and Propagation (EuCAP),2013.
- [18] Duman, T. and A. Ghayeb . Coding for MIMO communication systems,2007.
- [19] Liénard, M., et al. MIMO and diversity techniques in tunnels. 2014 International Conference on Computing, Management and Telecommunications,2014.
- [20] R. Janaswamy, *Radiowave Propagation and Smart Antennas for Wireless Communications*. KluwerAcademic Publishers, 2000.
- [21] L. C. Godara, *Handbook of Antennas for Wireless Communications*. CRC Press, 2002.
- [22] E. Telatar, "Capacity of multi-antenna gaussian channels," *European Trans. on Telecomm. ETT*,vol. 10, no. 6, pp. 585-596, 1999.
- [23] Eakkamol Pakdeejit, *Linear Precoding Performance of Massive MU-MIMO Downlink System*, A thesis of Linkopeng University, May 2013.
- [24] Long Zhao, Kan Zheng, Hang Long Hui Zhao and Wenbo Wang, Performance Analysis for Downlink Massive MIMO System with ZF precoding, *Transactions on Emerging Telecommunications Technologies*, Vol.8, no.3, 2014.
- [25] Yeon-Geun Lim, Chan-Byoung Chae, and Giuseppe Caire, Performance Analysis of Massive MIMO for Cell-Boundary Users, *IEEE Communication Magazine*, In Press, Available at: [http://arxiv:2309.7817v1 \[cs.IT\]](http://arxiv:2309.7817v1 [cs.IT]), 30 September 2013.
- [26] E. Björnson, M. Bengtsson, and B. Ottersten, "Optimal multiuser transmit beamforming: A difficult problem with a simple solution structure," *IEEE Signal Processing Magazine*, vol. 31, no. 4, pp. 142-148, 2014.
- [27] A. E. Forooshani, "Configuration of multiple input multiple output antenna arrays for wireless communications in underground mines," *The University of British Columbia, Vancouver, Canada*, Aug 2013.
- [28] Institute of Electrical and Electronics Engineers, "The IEEE standard dictionary of electrical and electronics terms"; 6th ed. New York, N.Y., Institute of Electrical and Electronics Engineers, c1997. IEEE Std 100-1996.

- [29] Southworth, G. C. (August 1936). "Electric Wave Guides" (PDF). *Short Wave Craft* 7 (1): 198, 233. Retrieved March 27, 2015.
- [30] A. Emslie, R. Lagace, and P. Strong, "Theory of the propagation of UHF radio waves in coal mine tunnels," *IEEE Trans. Antennas Propag.*, vol. 23, pp. 192-205, 1975.
- [31] Sun, Z. and I. F. Akyildiz. "Channel modeling and analysis for wireless networks in underground mines and road tunnels." *IEEE Transactions on Communications* 58(6): 1758-1768, 2010.
- [32] C. Briso-Rodriguez, J. M. Cruz, and J. I. Alonso, "Measurements and Modeling of Distributed Antenna Systems in Railway Tunnels," *IEEE Transactions on Vehicular Technology*, vol. 56, no.5, pp. 2870-2879, 2007.
- [33] D. G. Dudley, M. Lienard, S.F. Mahmoud, and P. Degauque, "Wireless propagation in tunnels," *IEEE Antennas Propag. Mag.*, vol. 49, pp. 11-26, 2007.
- [34] Forooshani, A. E., et al.. "Effect of antenna array properties on multiple-input-multipleoutput system performance in an underground mine." *IET Microwaves, Antennas & Propagation* 7,2013.
- [35] Z. Jimeng, X. Lei, G. Ke, and T. Yuanchun, "MIMO antenna configuration for LTE in railway," in 2017 15th International Conference on ITS Telecommunications (ITST), 2017.
- [36] P. Suvikunnas, J. Salo, L. Vuokko, J. Kivinen, K. Sulonen, and P. Vainikainen, "Comparison of MIMO Antenna Configurations: Methods and Experimental Results," *IEEE Transactions on Vehicular Technology*, vol. 57, pp. 1021-1031, 2008.
- [37] M. Lienard, P. Degauque, J. Baudet, and D. Degardin, "Investigation on MIMO channels in subway tunnels," *IEEE Journal on Selected Areas in Communications*, vol. 21, no. 3, pp. 332-339, 2003.
- [38] Institute of Electrical and Electronics Engineers, "The IEEE standard dictionary of electrical and electronics terms"; 6th ed. New York, N.Y., Institute of Electrical and Electronics Engineers, c1997.
- [39] P. V. Nikitin, D. D. Stancil, and E. A. Eroshva, "Estimating the number of modes in multimode waveguide propagation environment," in 2011 IEEE International Symposium on Antennas and Propagation (APSURSI), 2011, pp. 1662-1665.
- [40] Piera, F. J., and P. Parada. "On the Connections between Information and Estimation Theory: From Awgn Channels to Dynamical Systems with Feedback." Paper presented at the 2008 Information Theory and Applications Workshop, 27 Jan.-1 Feb. 2008 2008.
- [41] Pursula, Pekka, Timo Karttaavi, Mikko Kantanen, Antti Lamminen, Jan Holmberg, M. Lahdes, Ilkka Marttila, et al. "60-GHz Millimeter-Wave Identification Reader on 90-Nm Cmos and Ltcc." *Microwave Theory and Techniques, IEEE Transactions on* 59 (05/01 2011): 1166-73. <https://doi.org/10.1109/TMTT.2011.2114200>.
- [42] Rosenzweig, A., Y. Steinberg, and S. Shamai. "On Channels with Partial Channel State Information at the Transmitter." *IEEE Transactions on Information Theory* 51, no. 5 (2005): 1817-30. <https://doi.org/10.1109/TIT.2005.846422>.
- [43] Sandhu, S., and A. Paulraj. "Space-Time Coding for the Parametric Fading Channel-Capacity." Paper presented at the Conference Record of the Thirty-Third Asilomar Conference on Signals, Systems, and Computers (Cat. No.CH37020), 24-27 Oct. 1999 1999.

- [44] Wuyuan, Li, Zheng Xuehe, Yang Sen, Zhong Ning, and Lu Jihua. "A New Transmit Diversity Method Based on Waterpouring Principle in Multiple Antennas Systems." Paper presented at the The 2nd International Conference on Information Science and Engineering, 4-6 Dec. 2010 2010.
- [45] Yin, Xiaoyu, and Guoxin Zheng. "Experimental Investigation of Space and Polarization Characteristics of a Subway-Like Tunnel Channel." *Progress In Electromagnetics Research C* 83 (01/01 2018).